People`s Democratic Republic of Algeria

Ministry of Higher Education and Scientific Research

University of Echahid Hamma Lakhdar - El Oued

Faculty of Technology

Department of Electrical Engineering
Dissertation

ACADEMIC MASTER

Division: Electrical Engineering

Specialty: Electrical networks

Presented by:

- **Tayeb Hani**
- **Adel Houba**
- **Salim Messaoudi**

Entitled:

Surface Texturing of High Voltage Insultors: A Novel Approach for Performance Optimization

Dissertation Submitted in Partial Fulfillment of the Requirements for the Master

Degree in applied Sciences

Publicly defended in: 03/06/2024

Board of Examiners:

Dr. Guia Talal	**Supervisor**
Dr. Ali Khechekhouche	**Assistant Supervisor**
Dr. Mida Idris	**Chairman**
Dr. Gacem Abd El Malek	**Examiner**

Academic Year: 2023/2024


بسم الله الرحمن الرحيم

ACKNOWLEDGEMENTS

It is with great pleasure that we dedicate these lines as a sign of gratitude and deep appreciation to all those who, directly or indirectly, contributed to the realization and completion of this work. Above all, we thank Almighty God for helping me to accomplish this modest work.

We would like to thank ***Dr. GUIA Talal***, who kindly supervised us in the completion of this work and guided it from the very beginning. We thank her for her seriousness and efforts in helping, advising, and guiding us.

I also thank all the teachers in our department who have greatly contributed to our education

Finally, I would like to thank all the people who have participated, directly or indirectly, in the completion of this work.

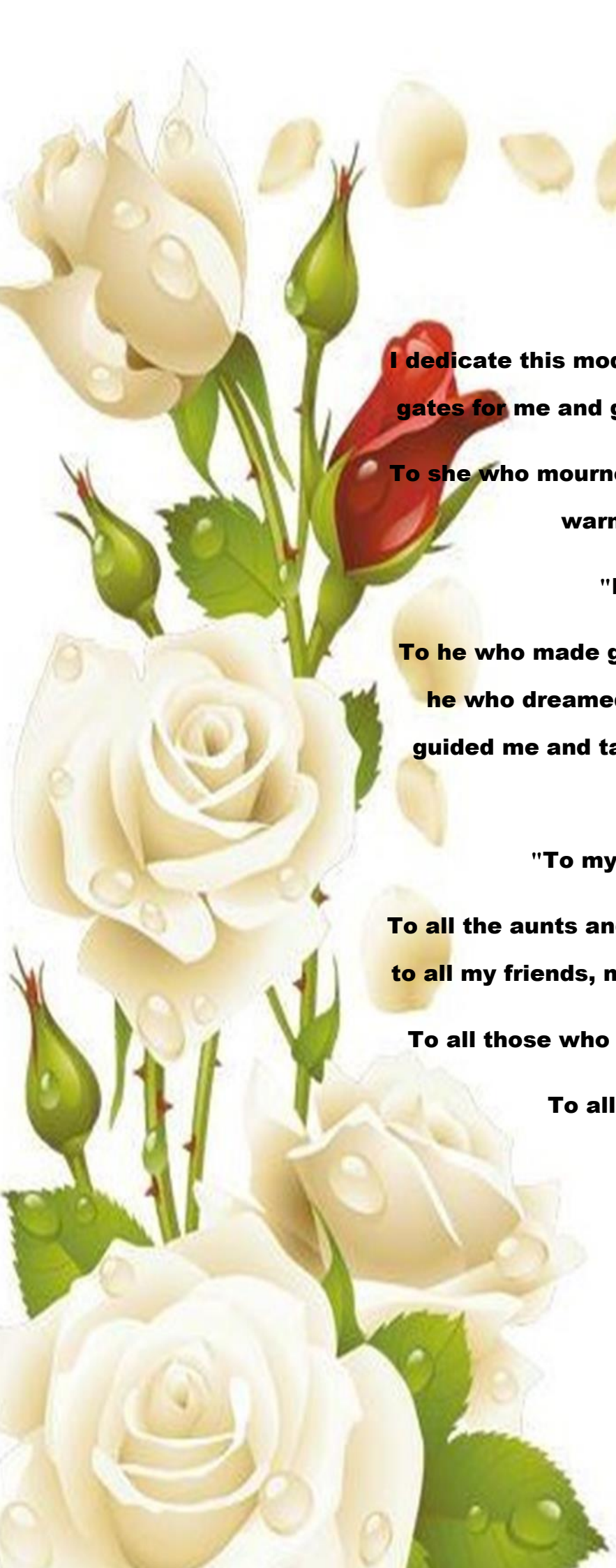

DEDICATIONS

I dedicate this modest work To she who opened the gates for me and gave me tenderness and courage

To she who mourned to make me happy To she who warmly awaits this day:

"My dear Mother"

To he who made great efforts for my happiness To he who dreamed of seeing this day To he who guided me and taught me the secrets of life "My Father"

"To my brothers and sisters"

To all the aunts and my uncle in the eternal life Also to all my friends, my wonderful brothers and sisters

To all those who helped me directly or indirectly.

To all my loved ones

TAYEB HANI

DEDICATIONS

In this honorable place, with a simple gesture traced in writing, but stemming from a deep feeling of gratitude, allow me to mention the names as a memorandum for those who hold a special place: To my dear father, to my dear mother, to my brothers and sisters, to all my cousins without exception,to all my family. To all my friends without exception.

To all, I dedicate this work, which is the culmination of my higher studies, as a heartfelt gift, praying to Almighty Allah to make it a service to our nation and to the well-being of humanity, and may it be a light on my professional path.

ADEL HOUBA

DEDICATIONS

In this honorable place, with a simple gesture traced in writing, but stemming from a deep feeling of gratitude, allow me to mention the names as a memorandum for those who hold a special place: To my dear father, to my dear mother, to my brothers and sisters, to all my cousins without exception,to all my family. To all my friends without exception.

To all, I dedicate this work, which is the culmination of my higher studies, as a heartfelt gift, praying to Almighty Allah to make it a service to our nation and to the well-being of humanity, and may it be a light on my professional path.

SALIM MESSQOUD

الملخّص:

في هذا العمل، ندرس تعزيز أداء العوازل عالية الجهد عن طريق إدخال تجويفات على سطحها. تمت دراسة العوازل البوليمرية المجوفة بالتجويفات النصف كروية من خلال الاختبارات المختبرية والتجارب الميدانية. تشير النتائج إلى تحسين في جهد الانهيار، وتقليل في كثافة التسرب الكهربائي، وتحسين في التوصيل الحراري مقارنة بالعوازل التقليدية. البحث الجاري يهدف إلى تحسين تصاميم العوازل المجوفة الموجهة لأنظمة النقل.

كلمات مفتاحية: عوازل عالية الجهد، تجويف السطح، العوازل البوليمرية، التجويفات النصف كروية، تفريغ التلوث، كثافة التسرب الكهربائي، التوصيل الحراري، أنظمة النقل.

Abstract:

In this work, we study enhancing the performance of high-voltage insulators by introducing surface texturing. Textured polymer insulators with hemispherical protuberances are investigated through laboratory tests and field trials. Results indicate improved breakdown voltage, reduced leakage current density, and better thermal dissipation compared to conventional insulators. Ongoing research aims to optimize textured insulator designs for transmission systems

Keywords: high-voltage insulators, surface texturing, polymer insulators, hemispherical protuberances, pollution flashover, leakage current, thermal dissipation, transmission systems.

Résumé:

Dans ce travail, nous étudions l'amélioration des performances des isolateurs haute tension en introduisant une texture de surface. Des isolateurs en polymère texturés avec des protubérances hémisphériques sont étudiés à travers des tests en laboratoire et des essais sur le terrain. Les résultats indiquent une amélioration de la tension de claquage, une réduction de la densité de courant de fuite et une meilleure dissipation thermique par rapport aux isolateurs conventionnels. Des recherches en cours visent à optimiser les conceptions des isolateurs texturés pour les systèmes de transmission.

Mots-clés: isolateurs haute tension, texture de surface, isolateurs en polymère, protubérances hémisphériques, pollution par flashover, courant de fuite, dissipation thermique, systèmes de transmission.

List of Figures

Chapter I: Previous studies on improvement performance of electrical insulators

Chapter II: Enhancing pollution performance of outdoor insulators using textured polymeric insulators

Chapter III: Experimental study and result

Appendix:

List of abbreviations and symbols

IPT: Inclined Plane Test

LC: Leakage Current

PD: Partial Discharge

ESDD: Equivalent Salt Deposit Density

RH: Relative Humidity FOV - Flashover Voltage

SIR: Silicone Insulator Rubber

TXT: Textured (insulator) CONV - Conventional (insulator)

HTV: High Temperature Vulcanized

ADE: Accumulated Dissipated Energy

NSDD: Non-Soluble Deposit Density

UV-B: Ultraviolet-B radiation

PLA+: Plastique (type of polymer)

HV: High Voltage

Db: Dry Band

DBA: Dry Band Arc

List of Tables

Chapter I: Previous studies on improvement performance of electrical insulators

Chapter II: Enhancing pollution performance of outdoor insulators using textured polymeric insulators

Chapter III: Experimental study and result

Appendix:

Summary

Chapter I: Previous studies on improvement performance of electrical insulators

Chapter II: Enhancing pollution performance of outdoor insulators using textured polymeric insulators

Chapter III: Experimental study and result

Appendix:

GENERAL INTRODUCTION

General Introduction

High and ultra-high voltage lines are the backbone of electricity transmission networks. Insulators are essential components in these systems, providing both mechanical support and electrical isolation. They support the high voltage-carrying parts and insulate them from the pylons.

During operation, insulators must withstand both normal and abnormal electrical stresses, such as transient over voltages, as well as environmental stresses like heat, rain, and ultraviolet radiation. Proper selection and sizing of insulators are critical to ensuring the reliability and quality of high-voltage insulation. The choice of insulating materials is among the key factors in their design, manufacturing, and operation.

In recent years, polymer insulators, also known as composite insulators, have gained widespread acceptance as substitutes for traditional porcelain or glass insulators due to their numerous advantages.

High-voltage insulators are continuously exposed to various environmental factors and contaminants, including natural and agricultural substances, as well as industrial emissions, during their service life. Insulators near coastal regions, for example, encounter sea salts, while those in urban areas are subjected to ash, dust, and chemical particles. These airborne particles tend to deposit and accumulate on the insulator surface, forming a layer that can become conductive when exposed to humid atmospheric conditions such as fog, mist, and drizzle. The presence of pollutants covering the insulator surface could also reduce the hydrophobicity of the polymer material, promoting the formation of a continuous conductive film. The leakage current resulting from system voltage generates resistive heating, which evaporates water from the wet surfaces, risking the formation of dry bands.

Several measures can be taken to enhance the performance of high-voltage insulators. Firstly, the use of innovative and more resistant materials, such as composites, can increase the resistance of insulators and their lifespan. Companies can also employ automatic cleaning systems or anti-adhesive

coatings to prevent contaminants from accumulating on the insulators. Improved designs can also be used to minimize disturbances to the electric field around the insulators and reduce the risks of electrical arcs.

Advanced monitoring technologies, like vibration and temperature sensors, can detect potential insulator damage and enable preventive interventions before failures occur. Lastly, regular training and increased safety awareness can help mitigate the risks associated with high-voltage insulators.

CHAPTER I:

PREVIOUS STUDIES ON IMPROVEMENT PERFORMANCE OF ELECTRICAL INSULATORS

I.1. Introduction:

The electrical insulator plays a crucial role in many applications, ensuring effective separation of electrical conductors to prevent unwanted current leaks. The performance of these insulators largely depends on the quality of their surface. A well-treated surface contributes to electrical stability, resistance to discharges, and overall durability of the insulator.

In the presence of humidity, various pollutant deposits become more or less conductive, and leakage currents establish themselves on the surface of the insulators. Once these currents reach a certain intensity, the conductive layer dries out in areas of high current density. This results in a modification of the potential distribution and electric fields, leading to the formation of small electrical arcs on the insulating surface, which can eventually develop into complete bypassing of the insulators.

Several approaches can be used to improve the performance of insulators. In this chapter, we will focus on some studies in this field.

I.2. High Voltage Insulator

The insulator is a solid insulating material capable of withstanding electrical stress. It is characterized by a high impedance to the passage of electric current. Its role is to separate two conductive bodies, subjected to different potentials, in order to prevent short circuits, current losses, and the risk of electrocution [1].[2]

Insulators in overhead lines have two main functions. On the one hand, they electrically isolate the power transmission lines from the grounded pylons, and on the other hand, they have a mechanical role which is to support these same lines and therefore resist the various mechanical stresses mainly due to the weight of the line, its movement in the presence of wind, etc. [3]

I.3. Previous studies on improving the performance of electrical insulators.

I.3.1. Definition of performance optimization of high voltage insulators

We can define the improvement of high voltage insulator performance as the process of enhancing their electrical and mechanical properties to increase the efficiency, reliability, and safety of high voltage power transmission and distribution networks. This improvement can be achieved through research in materials science, optimization of design, performance evaluation regarding pollution, and testing under various conditions. The goal is to ensure that high voltage insulators can withstand extreme weather conditions, resist pollution, prevent bypassing, and maintain stable electrical insulation properties throughout their lifespan. Optimization can be done through various means, such as improving the performance of outdoor insulators installed in coastal areas using a silicone rubber

coating [4], and enhancing the withstand voltage performance in the presence of pollution for cylindrical porcelain insulators [5].

I.3.2. Distribution of Leakage Current on Polymer Insulator Surface

Yong Zhu et al. [6] utilized information provided by the leakage current signal to characterize the surface condition of a SIR (Silicone Insulator Rubber) insulator and to compare the results with those from a proposed model. Diagnostic analysis based on the leakage current signal was taken into consideration. This study also accounted for the behavior of electrical discharges occurring on the surface of polymers:

• Local arcs occurring in dry bands.

• Partial discharges caused by the triple junction between water droplets, polymer, and air due to the difference in their permittivity [7].

• The experimental model took into account pollution by humidity, as it is widely used in research to study the electrical performance of polymers under high voltage [8].

• Real insulator pollution and its model shown in Figure I.1 are done with a solution of 3 liters of distilled water containing 12 g/l of NaCl; measurements conducted with the ESDD indicate 0.03 mg/cm2 for this solution. Surface pollution is done through spraying. We use a camera to observe the discharge phenomenon and an oscilloscope connected to a computer to record leakage current signals. Additionally, using the finite element method, we evaluate the electric field and identify areas with high intensity [9].

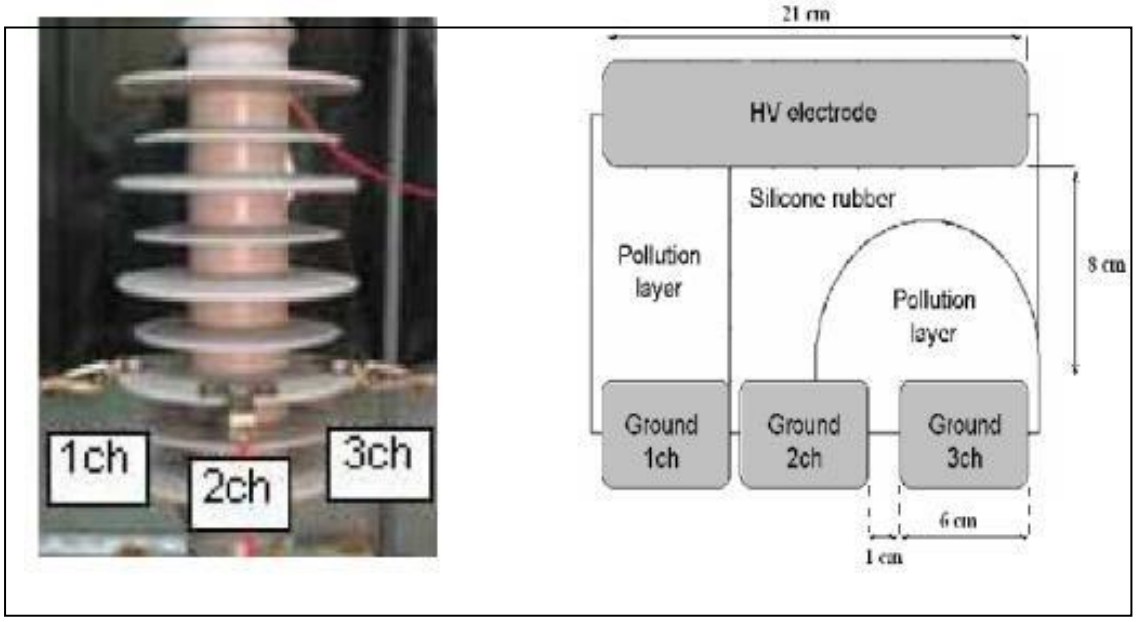

Figure I.1. Real insulator (on the left) and its model (on the right).

The results obtained from the analysis of currents 1ch, 2ch, and 3ch show that 1ch has a perfectly sinusoidal shape due to the uniformity of the pollution layer (perfectly resistive nature); 2ch and 3ch have a distorted shape due to both the intense discharge activity and the non-uniformity of the pollution layer (see Figure I.1). The observed discharges are caused by an electric field whose value exceeds the dielectric strength of the system in question.

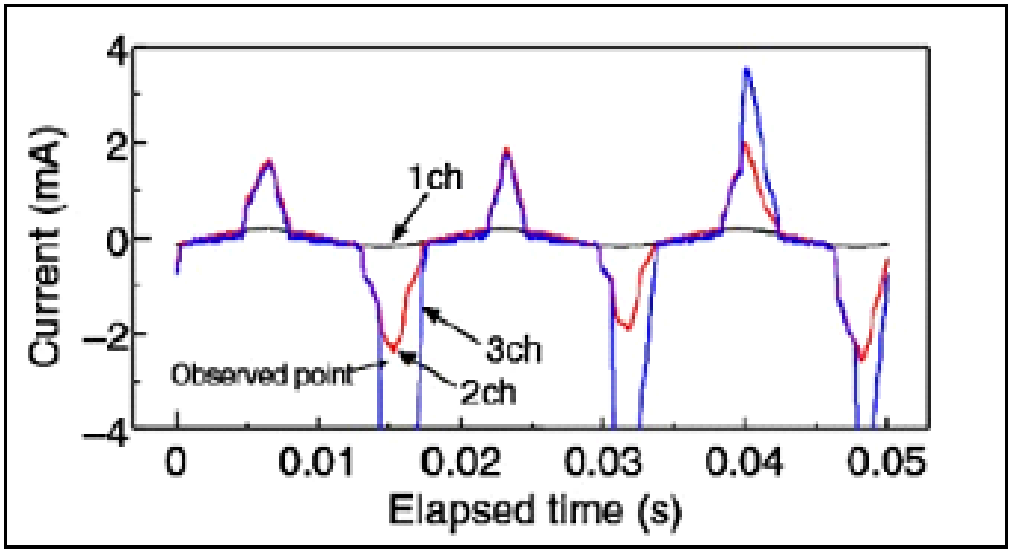

Figure I.2. Waveforms of leakage currents from the model.

In the case of the real insulator, all three leakage current signals exhibit distorted waveforms. This distortion is due to the irregularity of the insulator profile. The occurrence of local arcs, caused by the drying out of certain areas, contributes to this situation, resulting from an uneven distribution of leakage current.

Monitoring discharge activity via camera allowed for the detection of their positions concerning the amplitude variation of 1ch, 2ch, and 3ch:

- A discharge appears at 37 ms on 1ch.

- The movement of this discharge from 1ch to 2ch at 38 ms is characterized by an increase in the amplitude of current 2ch.

- The appearance of the discharge between 2ch and 3ch after 1 ms increases the amplitudes of currents 2ch and 3ch [9].

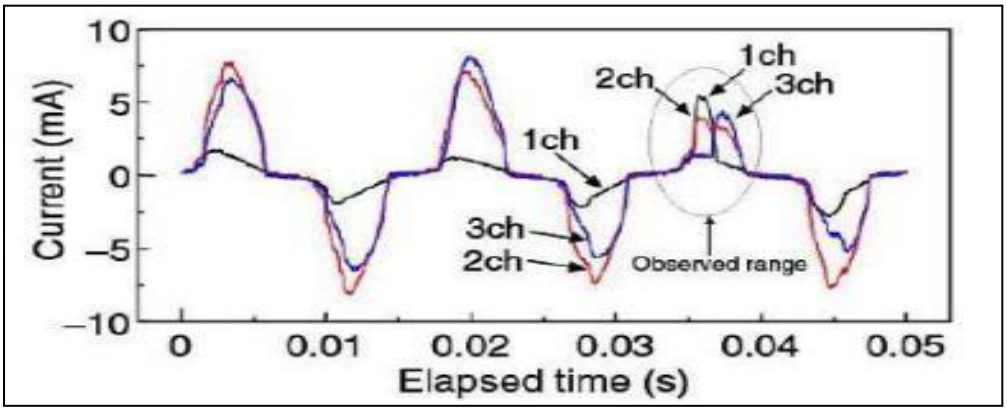

Figure I.3. Waveforms of leakage currents of the actual insulator.

It can be deduced from this study that the leakage current can serve as a means of detecting the positions of partial discharges and can identify the surface condition of the insulator.

I.3.3. Temporal and Frequency Analysis of the Leakage Current Signal from an Insulator Covered with Ice

F. Meghnefi et al [10] focused on analyzing the leakage current (LC) signal of a porcelain insulator covered with ice. The results obtained show that the leakage current signal during ice accumulation is characterized by specific waveforms and harmonic frequencies. Laboratory tests also showed that analyzing this signal allows for estimating the ice accretion rate. This is possible by studying the time evolution of the 1st, 3rd, and 5th order harmonics as well as the phase shift between the applied voltage and the leakage current signals. Ice formation was simulated artificially in a cold room measuring 6m×6m×9m specially designed for such research. The ice was formed from supercooled droplets produced by a nozzle system, as shown in Figure I.4. High voltage supply is ensured by a high-voltage test transformer (350 kV). The leakage current signal is recorded through a 5Ω shunt.

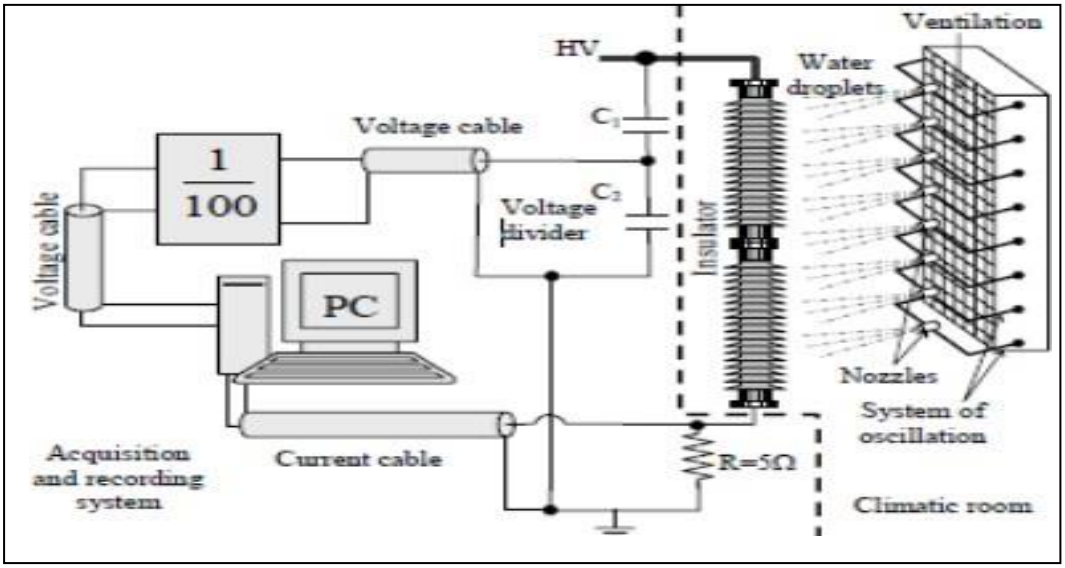

Figure I.4. Experimental setup.

To monitor the surface condition of the insulator under the effect of ice, the authors studied the variations in the harmonics of the leakage current signal, focusing on those of orders 1, 3, and 5 (60Hz, 180Hz, and 300Hz). For a better representation, the amplitudes of the 3rd and 5th order harmonics are plotted relative to that of the fundamental in Figure I.5.

The authors deduced that initially (with low ice deposits), the amplitudes of both harmonics are low compared to that of the fundamental, confirming that the leakage current remains sinusoidal during this period. Furthermore, the same researchers were able to conclude that studying the phase difference between the applied voltage and the leakage current is of paramount importance because it allows estimating the accumulation of ice on the insulators. This phase difference increases with the accumulation of ice [9].

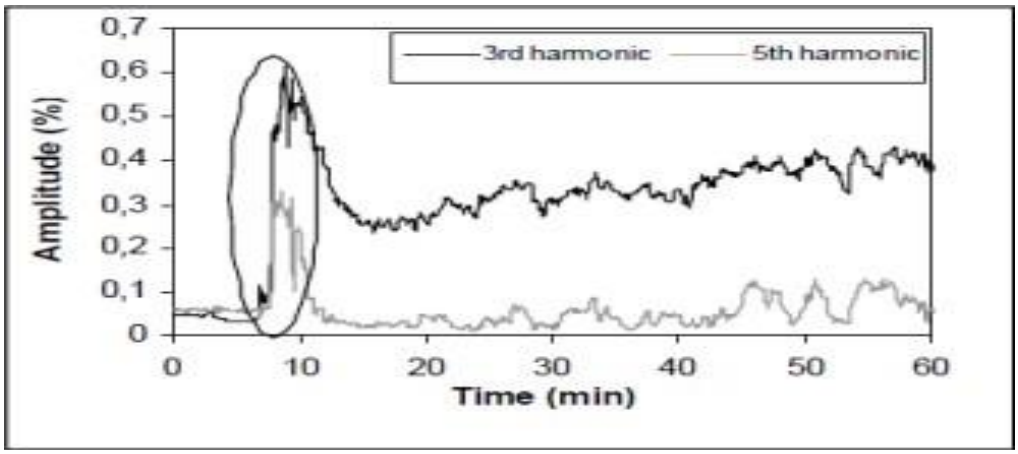

Figure I.5. Evolution of the ratio of the 3rd and 5th order harmonics to that of the fundamental of the leakage current signal.

I.3.4. Determination of the probability of occurrence of flashover of composite insulators using the harmonic components of the leakage current signal.

H. H. Kordkheili et al [11] proposed a new method to predict the flashover of Silicon Rubber (SIR) insulators and its probability of occurrence by analyzing the harmonic components of the leakage current signal. The tests were conducted on samples of insulators polluted with different profiles. (Figure I.6-Table I.1).

Table I. 1. Characteristics of the insulators.

Insulator N°.	1	2	3	4	5
Nominal voltage (kV)	34	24	24	24	24
Length of the insulator string (mm)	720	520	520	449	449
Creepage distance (mm)	1070	770	590	674	630

Figure I. 6. Tested insulators.

To verify the effectiveness of their new method, these researchers conducted leakage current measurements on different insulators, at various humidity levels and different contamination levels. The results of these measurements for insulator No. 1 are presented in Figure I.7.

H. H. Kordkheili et al [11] showed that when the amplitude of the 5th harmonic component is greater than that of the 3rd harmonic, this means that the insulator is clean or very lightly polluted. The researchers also found that if flashover does not occur at the beginning of humidification, it will not occur at humidity saturation either. In the same study, the researchers demonstrated that the variation of the ratio between the amplitudes of the fifth and third harmonics is a very reliable indicator for evaluating the surface condition of a specific insulator [9].

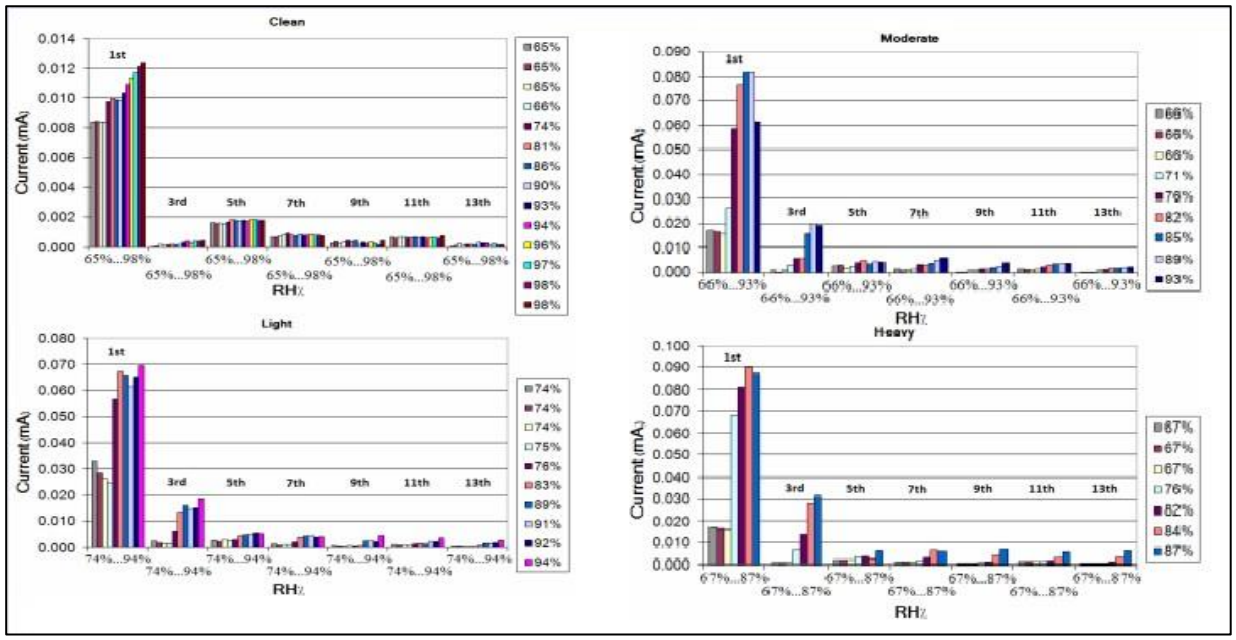

Figure I.7. Variation of the amplitude of the leakage current harmonics for different humidity levels and contamination levels.

$$K_{5/3} = \frac{Amplitude\ of\ the\ 5th\ harmonic}{Amplitude\ of\ the\ 3rd\ harmonic}$$

According to tests conducted in the same laboratory, researchers observed that under normal service conditions, the K5/3 index is greater than 100%. Therefore, they concluded that if this condition is met, the flashover is very unlikely. Additionally, they also noticed that for all cases where flashover occurs, the K5/3 index is less than 30%. Thus, they deduce that recognizing an insulator with a K5/3 index less than 30% is a necessary but not sufficient condition. They demonstrate that the probability of flashover occurrence in this latter case is 90% [11].

I.3.5. Analysis of partial discharges for the diagnosis of the surface condition of polymer insulators.

In order to estimate the severity of pollution on line insulators, S. Chandrasekar et al [12] analyzed partial discharges on Silicone Rubber (SiR) insulators. Tests were conducted on several samples (see Figure I.8) under alternating voltage with different levels of pollution and relative humidity (RH) [9].

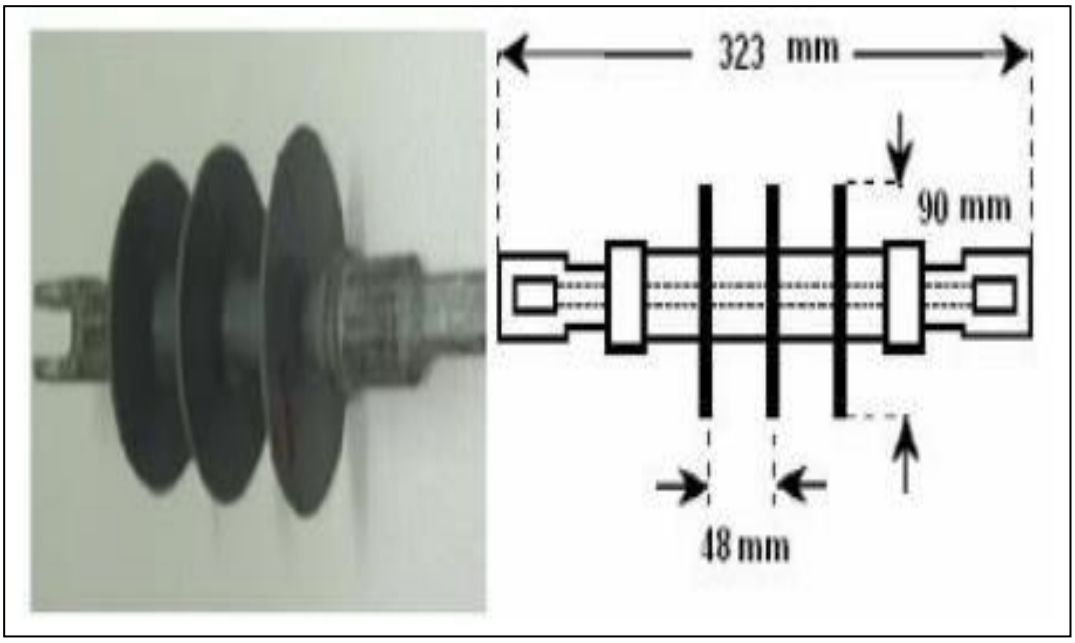

Figure I.8. Photograph and diagram of a 11 kV SiR sample.

The insulators are suspended in a chamber (1.5 m × 1.5 m × 1.5 m) where fog (NaCl) is injected to vary the ESDD in mg/cm2 from 0.06 to 0.25. For this experiment, the setup used is shown in Figure I.9.

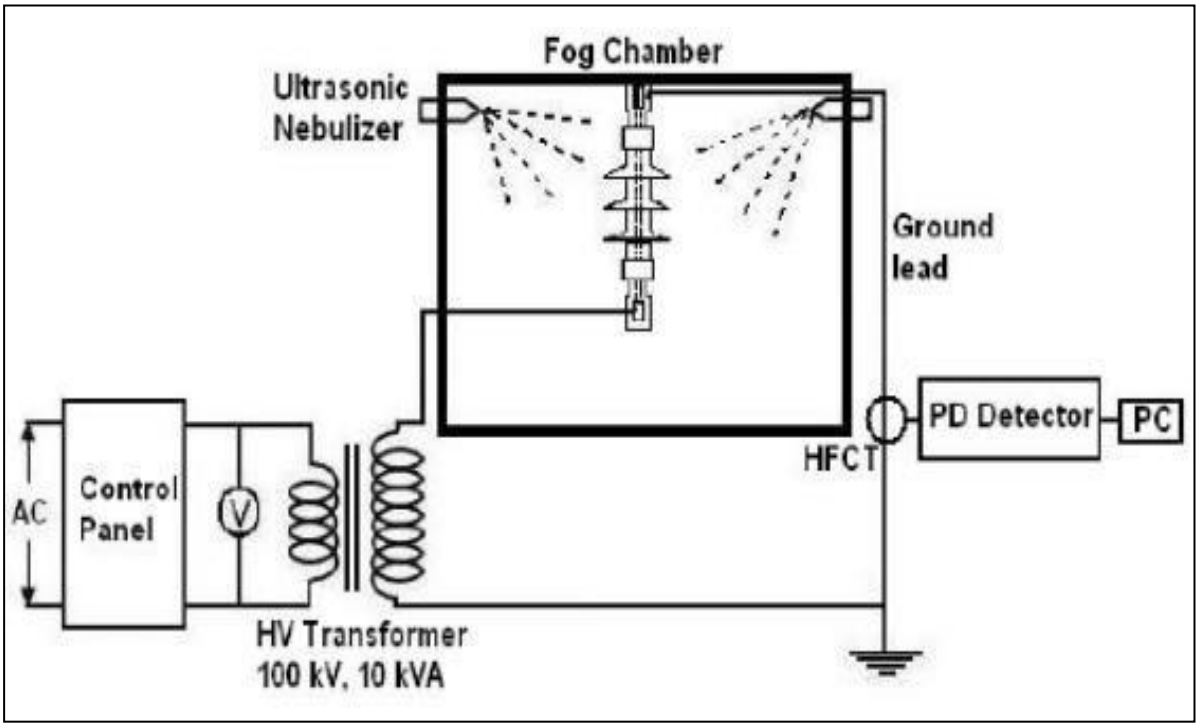

Figure I.9 Experimental setup.

Several tests were conducted:

- Tests on a clean SiR insulator, under different relative humidity levels (30 to 40%);
- Tests on a SiR insulator (ESDD = 0.08 mg/cm2, RH = 60 to 100%);
- Tests on an insulator (SiR) at RH = 100%, (ESDD ranging from 0.06 to 0.25 mg/cm2). For clean insulators, the authors noted the absence of partial discharges. For a pollution level of 0.08 ESDD, and a relative humidity ranging from 60 to 100% (see Figure I.5), the authors observed that:
- The amplitude of the PD increases with the increase in RH;
- For low RH (60% to 80%), the dominant frequency components of the PD signal are in the 6-25 MHz band;
- For high RH values (above 90%), the frequency components are in the 2-6 MHz band.

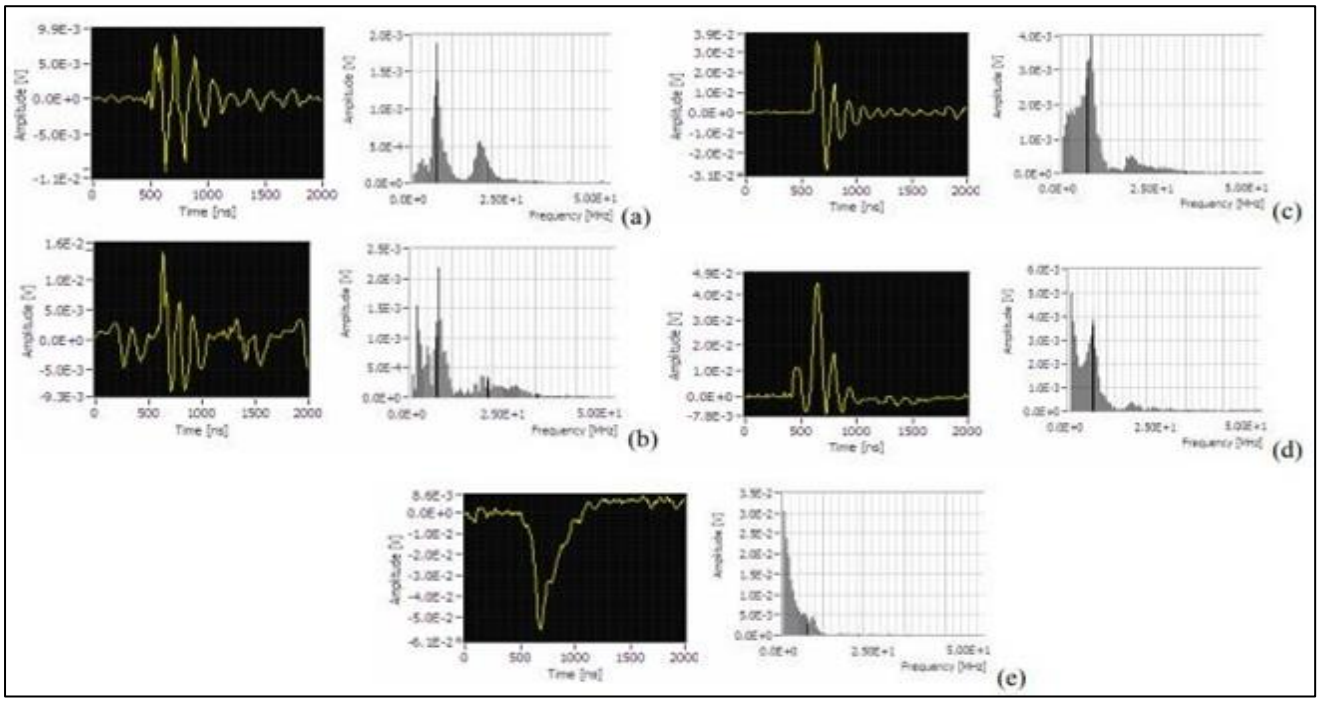

Figure I.10. Signals obtained (temporal and frequency representations) of the PD at 0.08 ESDD: (a) 60%RH, (b) 70%RH, (c80%RH, (d) 90%RH, (e) 100%RH.

For a pollution level ranging from 0.06 ESDD to 0.25 ESDD with RH=100% (see Figure I.9), the authors concluded that as the pollution level increases:

- The amplitudes of the PD increase;
- The repetition rate (occurrence of all PD within a specific time) decreases;

- The amplitudes of the frequency components increase in the 1-6 MHz band.

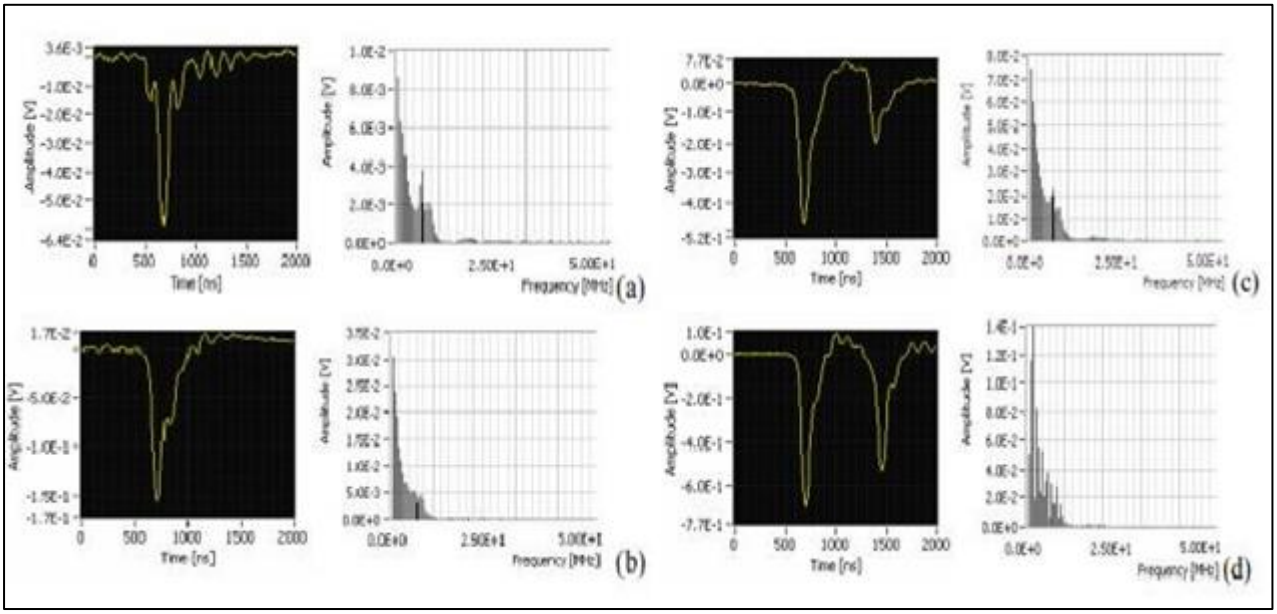

Figure I.11. Signals obtained (temporal and frequency representations) of the PD for RH=100%: (a) 0.06 ESDD, (b) 0.08 ESDD, (c) 0.12 ESDD, (d) 0.25 ESDD.

By analyzing the results and graphs obtained, the authors concluded that the asymmetry value of the PD signal decreases significantly with increasing pollution under high pollution conditions. However, they estimated that using this parameter alone is not sufficient to diagnose the insulator's condition. This study was completed by a statistical analysis, with parameters including the shape parameter β and the average phase of the PD signal, for different ESDD and RH values. The variation of the β parameter and the average phase prove to be a good tool for diagnosing the severity of pollution [9].

I.3.6. The use of booster sheds to improve the performance of 800 kV multicone type insulators under heavy rain.

In previous studies, [13] proposed a method to improve the performance of insulators. High voltage flashover tests were conducted at the CEPEL HT laboratory, under 60 Hz AC voltage, using two cascade test transformer units capable of applying a voltage up to 900 kV and 2 amperes. Initially, the tests aimed to determine the appropriate number and position of booster sheds (BS) for each complete insulator column (two insulator sections assembled in series). This experiment was conducted based on UV images associated with discharge activities along the insulator when subjected to high voltage under heavy rain. Subsequently, tests were performed on insulator sections to quantify the effectiveness of BS in improving the insulator performance in case of flashover. In all cases, tests were

conducted on insulators with and without BS, and the results were compared under the same test conditions; dry or wet conditions with artificial rainfall of 5 mm/min; water resistivity being 100m.

For the flashover tests on the complete insulator column, the withstand voltage level of 885 kV was verified, with the voltage applied for one minute after a 15-minute pre-humidification time. For tests on insulator sections, the flashover voltage was determined as an average value of five or ten breakdown voltages (Ud), depending on the dispersion of the Ud values. The artificial rainfall structure and other non-active metallic parts inside the test area were kept as far away as possible from the active components of the test circuit, with the minimum distance being about 12 m. The precipitation rate and the uniformity of the artificial rain along the insulator under test were measured and verified according to the standardized procedure. The dimensions of the metallic structure used as a physical base for the insulator under test and its height above the laboratory floor were established as closely as possible based on a real insulator arrangement on a 765 kV substation bus. Examples of test arrangements used are presented in Figure I.12.

Figure I.12. Examples of test circuit arrangements. Insulator column at the end of a busbar (a) with and (b) without BS; insulator column in the middle of a busbar (c) without BS; and insulator section without BS (d).

- ✓ **Results**

During the tests conducted with different quantities and positions of Booster Sheds (BS) along the insulator column, it was observed that both the appropriate quantity and position of BS must be considered to find the best configuration to improve its flashover performance under heavy rain conditions.

Investigations were carried out with BS positioned uniformly every three to seven sheds along the insulator, as well as with some non-uniform BS distributions. The most appropriate BS configuration was defined based on UV images and was not the same for insulators from manufacturers "A" and "B", as shown in Figure I.13. For manufacturer "A", eight BS positioned every five sheds from top to bottom of the insulator column were found to be the best configuration. For manufacturer "B", six BS distributed non-uniformly as shown in Figure I.13 were the most suitable. A schematic representation of the selected BS configurations for the two insulator columns is presented in Figure I.14.

Each insulator was tested with the selected BS configuration under artificial rainfall of 5 mm/min, 885 kV, proving its withstand capability in two different test arrangements: in the middle and at the end of a typical 800 kV busbar. When tested without BS, the insulator column failed in some cases, mainly when the arrangement represented the end of the busbar under 5 mm/min conditions. The insulators used in these experiments, without BS, were also tested strictly according to current standardized procedures for wet tests and proved their withstand capability under artificial rainfall of 1 mm/min.

The improvements in the flashover performance of the complete insulator columns through the use of BS were verified using UV images, as shown in Figure I.13. The UV images were very useful during the investigation, allowing the evaluation of the flashover performance of insulators based on the intensity, extent, and location of discharge activities. It was possible to observe, for example, that the withstand capability of the insulator was very unstable in some tests without BS, despite not having completely flashed over. [21]

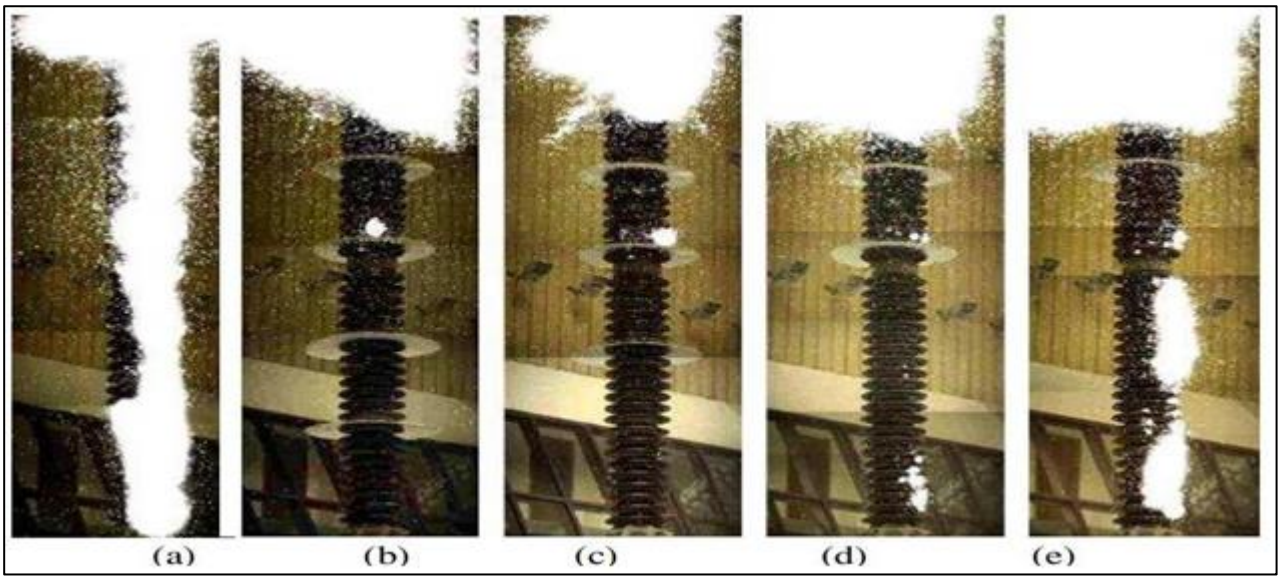

Figure I.13. UV images for an 800 kV multicone type insulator, manufacturer B, under 885 kV, artificial rainfall of 5 mm/min. (a) without booster sheds (BS); (b) 6 BS: sheds 2, 9, 14, 21, 28, and 35; (c) 5 BS: sheds 2, 9, 14, 21, and 28; (d) 4 BS: shed

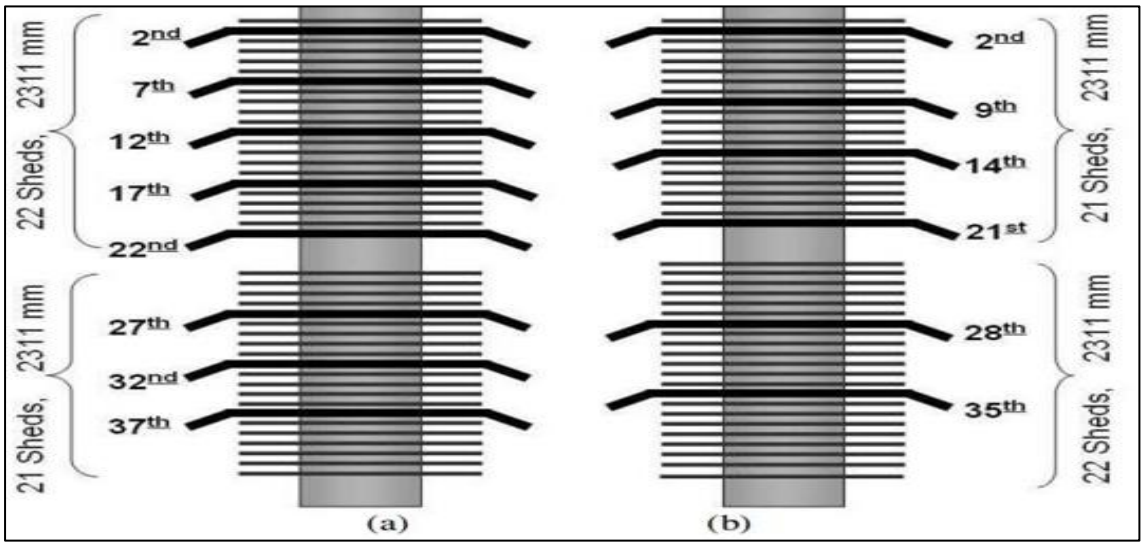

Figure I.14. Schematic drawing of the BS configurations on the insulator column from manufacturer "A" (a) and manufacturer "B" (b).

I.3.7. Improvement of flashover performance in the presence of pollution for porcelain cylindrical insulators

In previous studies, [5] proposed a method to improve the performance of insulators in terms of pollution flashover voltage. The four types of insulator specimens were fundamentally evaluated by the standard salt fog test procedure specified in publication IEC 60507, except for the salt fog flow rate. The flow rate was reduced by half from the specified value (500 cc/min/nozzle), taking into account the correlation between laboratory and field test results of polymer insulators. Additionally, the preconditioning prescribed in the IEC standard for the salt fog test of conventional porcelain and glass

insulators was not performed, as this could destroy the hydrophobicity of silicone rubber-coated surfaces. Only the bare porcelain surfaces of the samples were carefully washed with detergent before individual tests. A sample was installed vertically in the test chamber and energized with a test voltage. The salt fog was then directly sprayed onto the sample insulator from both sides. Flashover or withstand for one hour was confirmed. The test was then repeated on another clean sample, applying the voltage one step lower or higher based on the results of the previous test. The 50% flashover voltage was determined by the up-down method after obtaining 10 or more effective data points. The power source used in this study was sufficiently rigid to evaluate pollution flashover voltages of insulators even under heavy pollution conditions.

✓ **Test Results**

The results of measuring the surface resistance of individual sheds along the silicone rubber-coated insulators, only on all sheds and without any coating on the entire insulator surface, are presented in Figure I.15. In the case of the sample with coating on the sheds, although the measurements were performed separately for the upper and lower surfaces of the sheds, the difference in surface resistance between the upper and lower surfaces of the sheds is generally not significant. In the case of the sample without coating, although the combined resistances for the upper and lower surfaces of the sheds are presented in Figure I.15, they are mainly lower compared to the separate values for the upper and lower sheds of the coated shed sample. In the case of the coated shed sample, except for a few limited sheds, most sheds have almost identical higher surface resistances compared to the bare porcelain surfaces. Thus, the voltage applied to the entire sample insulator with shed surface coating is considered to be divided and allocated to these individual sheds. [21]

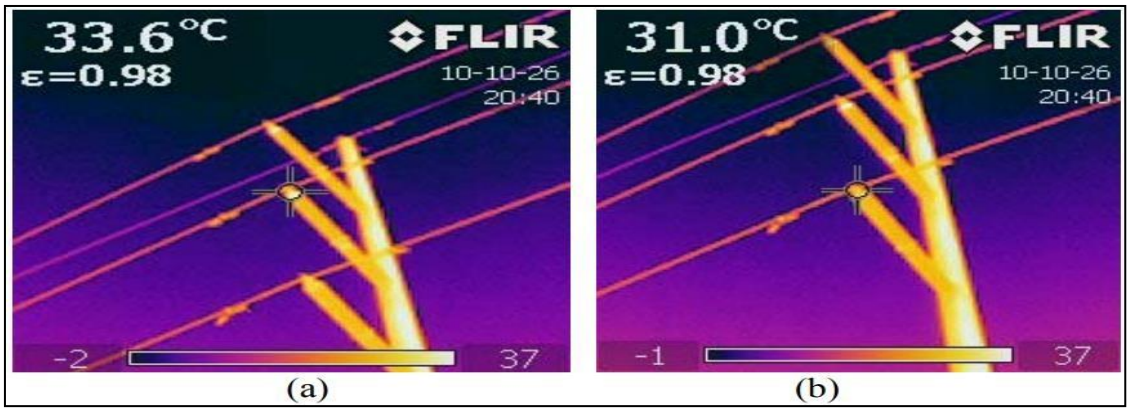

Figure I.15. Infrared temperature image for (a) an uncoated insulator and (b) a coated insulator at Ketewel beach.

On the other hand, in the case of the bare porcelain insulator without any coating, over time, only a small number of limited sheds have much higher resistance compared to the other sheds, suggesting the formation of dry bands resulting from the concentration of voltage stresses on these sheds with higher resistance. In fact, as typical discharge activities are presented in Figure I.16, the three samples with partial or full silicone rubber coating show partial discharge activities on almost the entire sample surface, indicating a uniform voltage distribution along the insulator, while the sample without coating shows only discharge activities limited to the upper part, indicating a very non-uniform voltage distribution.

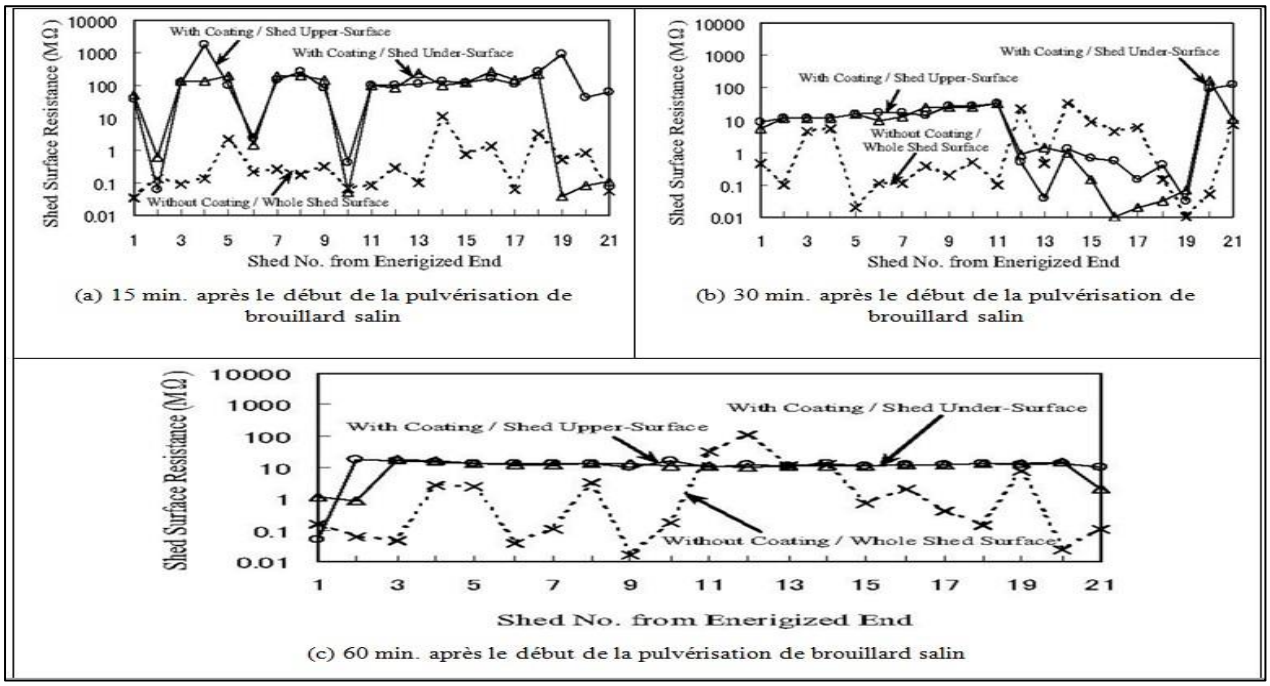

Figure I.16. Distribution of surface resistance of sheds along the insulator.

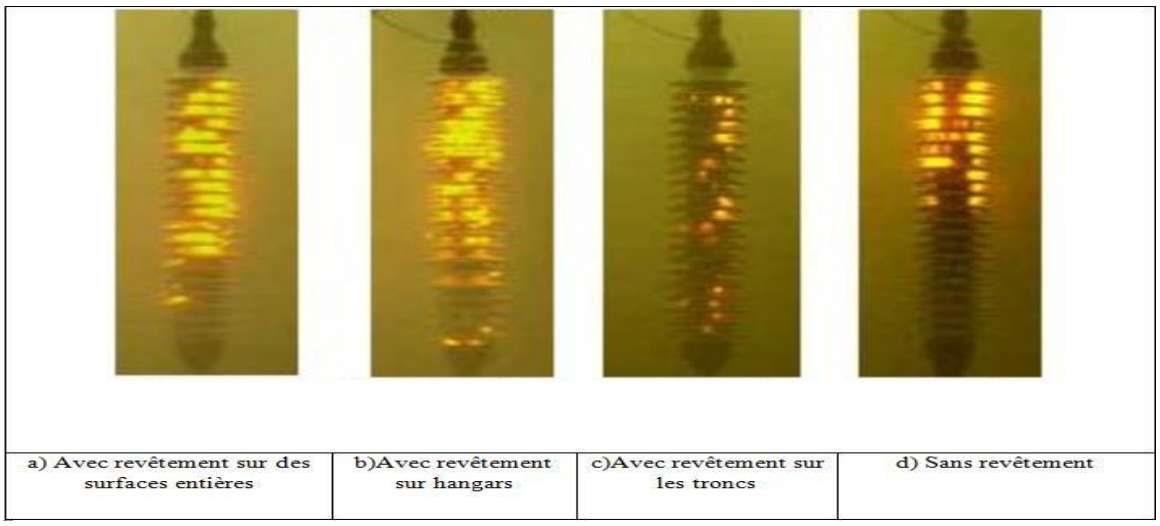

Figure I.17. Discharge activities.

I.4. Conclusion

The development of research in the field has provided access to several new technologies that contribute to enhancing the credibility of an electrical system. The most effective current methods for assessing the severity of insulator pollution are practically based on the application of signal processing methods on the leakage current wave. These results, along with previous work in this chapter, inspire us to apply these methods in the field of high voltage, especially for improving insulator performance.

CHAPTER II:

Enhancing Pollution Performance of Outdoor Insulators Using Textured Polymeric Insulators

II.1. Introduction

Polymeric insulators have shown advantages in polluted environments but still face challenges such as pollution performance. To address this, textured insulator surfaces with hemispherical protuberances have been proposed, leveraging silicone rubber's melding properties. These textures aim to improve dry banding distribution and flashover performance. Extensive investigations and collaborations have led to successful laboratory tests demonstrating the superior performance of textured insulator surfaces. An industry-funded project is underway to develop and trial these textured insulators on transmission systems up to 400 kV, with a focus on evaluating 400 kV insulator prototypes. This chapter presents the results of laboratory testing and ongoing research, highlighting advancements in textured insulator design and manufacturing for improved pollution performance in outdoor insulation systems.

II.2. Challenges in Polymeric Insulator Design

Designing polymeric insulators poses numerous challenges due to their unique properties and environmental requirements. Key challenges include material selection, hydrophobicity maintenance, surface tracking, creepage distance optimization, mechanical design, texture and profile design, and testing compliance. Addressing these challenges necessitates a multidisciplinary approach involving various fields such as materials science, electrical and mechanical engineering, and polymer chemistry to ensure the development of efficient and reliable polymeric insulators for diverse applications.

II.3. Texturing of polymeric insulators

The extensive use of polymeric materials, and especially hydrophobicity transfer materials like silicone rubber for composite insulators, did not lead to the total elimination of pollution flashover. Severe ambient conditions would still result inpartial discharging on the insulator surface and the design of polymeric insulators remains very simple mainly due to the molding restrictions inhibiting the development of re-entrant profiles [14].

The surface leakage current on a polluted polymeric insulator has the highest density in the regions of the smallest contour perimeter which are the shank sections. Consequently, the surface electric field strength is also at its highest at these regions resulting in increased surface power dissipation. Heating is proportional to the power dissipation. Therefore, local heating leads to the formation of dry-bands and the damaging effect induced by the associated surface discharges.

Textured insulators are a novel approach [15] for the design of polymeric insulators that takes advantage of the moulding properties of silicone rubber. Fine texturing of the polymeric surface

could be achieved by employing a pattern consisting of an array of contiguous or overlapping protuberances. The aim of this design is to reduce the surface power dissipation by reducing both the electric field and current density. This could be achieved by increasing both the surface area and the creepage distance of the insulator without increasing the overall longitudinal length of the insulator [14]. Moreover, textured patterns were expected to alleviate the damage induced on polymeric materials due to surface discharges, compared with non-textured samples of the same material, by introducing multiple paths for current conduction: as soon as one current path starts to dry as a result of Joule heating, its resistance will increase. However, the current flow will switch to an alternative path of lower resistance before severe thermal damage occurs [14].

II.3.1. Surface patterns

The geometry of such protuberances could be hyperboloidal, conical and pyramidal or other symmetrical shapes each resulting in a different variation of the surface area [14].

Figure 1 shows a side view of a protuberance that is formed as part of a sphere and has a height, c, and a base as a circle of radius, a. The radius of the sphere is b. Also, the top view of an array of contiguous part-spherical protuberances is shown (Figure 1b).

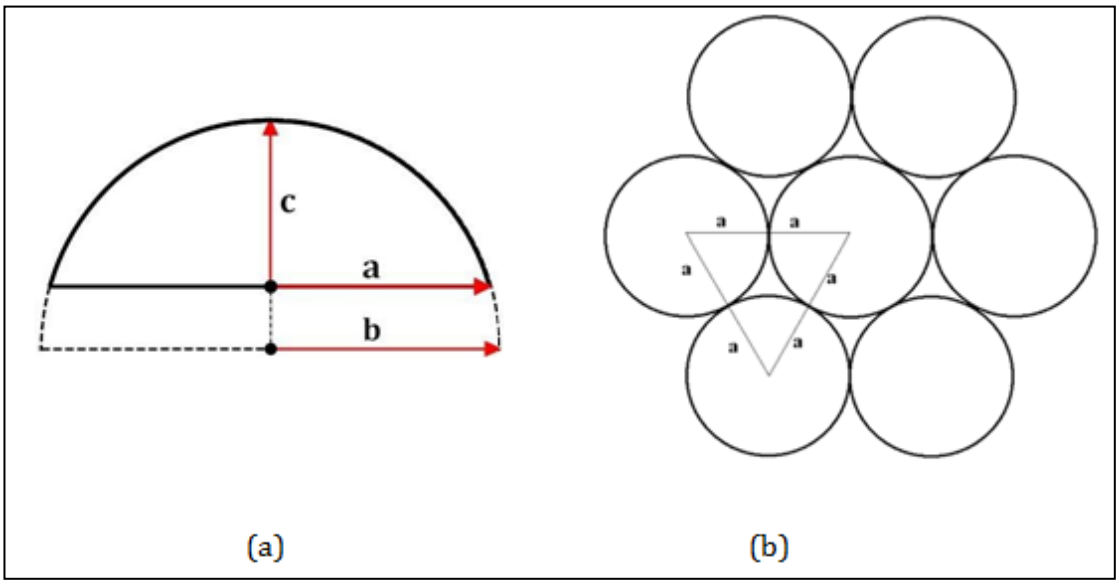

Figure II.1. Side view of part-spherical protuberance (a) and top view of an array of contiguous part-spherical protuberances (b) [14].

Therefore, we can write

$$a^2 = c\,(2b - c) \qquad (1)$$

and the surface area of the spherical cap will be

$$A_p = 2\pi bc \quad (2)$$

From Figure 1-b, the area of the triangular plane surface is

$$A_t = \sqrt{3}a^2 \quad (3)$$

The three neighbouring protuberance will increase this surface area to

$$A_{pt} = \frac{Ap}{2} + A_t - \frac{\pi a2}{2}$$

$$A_{pt} = a^2[\frac{\pi b}{2b-c} + \sqrt{3}-\frac{\pi}{2}] \quad (4)$$

Therefore, the spherical protuberances will increase the surface area by a ratio

$$\frac{A_{pt}}{A_t} = 1 + \frac{\pi c}{2\sqrt{3}(2b-c)} \quad (5)$$

Equation (5) is suggesting that, for protuberances that are formed as part of spheres, the increase of the surface area is dependent on the height of the sphere cap and on the radius of the sphere. If the protuberance is a hemisphere (b=c) then the ratio for a contiguous hemispherical pattern will be

$$\frac{A_{pt}}{At} = 1 + \frac{\pi}{2\sqrt{3}} = 1.907 \quad (6)$$

which is independent of the hemisphere radius b. For a tightly arranged array of adjacent hemispherical protuberances, the surface will increase close to a limiting value of 2, which is the ratio of the hemisphere surface to the surface of the circular base. Ratios greater than 2 can be achieved by utilising other geometrical arrangements [15].

The typical approach for the design of outdoor insulators for polluted environments is the increase of the creepage distance per unit of axial length. The textured patterns aim to achieve both longer creepage and an increase of the surface area. For hemispherical protuberances, intersections. Figure 2 shows such geometrical configurations along with the contiguous pattern (Figure 2-A). The arrows indicate the circular arc paths formed by the intersections. Pattern B follows a hexagonal intersection of overlapping hemispherical protuberances while the intersections of patterns C and D have a square and triangular shape respectively [15].

Returning to the example of the contiguous hemispherical protuberances pattern (Figure 2-A),

the creepage distance per row in the direction of the electric field is 2.093a while the distance on the plane surface is √3a, marking an per unit increase of the creepage distance by a factor of 1.209, resulting in a substantial decrease of both *E* and *J* [15]. The creepage factor is also independent of the hemisphere radius.

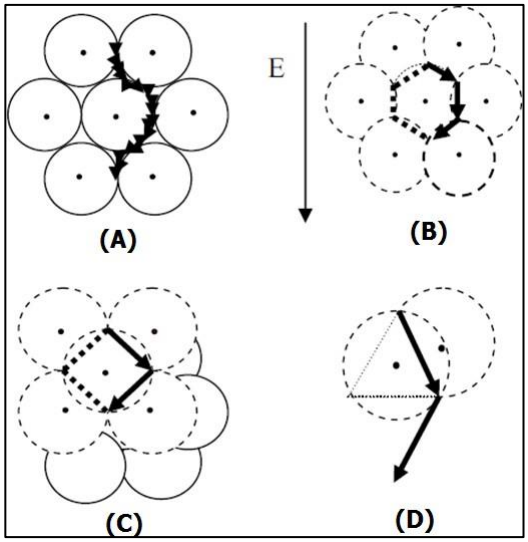

Figure II.2. Textured patterns: contiguous hexagonal (A), intersecting hexagonal (B), intersecting square (C) and intersecting triangular (D) [15].

II.3.2. Power dissipation factor

Assuming that the plain and textured surfaces are covered by a pollution layer of same thickness *t* (metres) and conductivity *σ* (Siemens/metre), then the layer conductance is $k = t \cdot \sigma$ *(*Siemens) and is the same for both surfaces. For an insulator leakage current, *I*, at position where the insulator circumference is *C* (metres) the current density inside the pollution layer is $J_{layer} = I/Ct$ (A·m^{-2}). As the thickness of layer *t* is constant, this can be expressed as a surface current density $J = J_{layer} \cdot t$ (A·m^{-1}).

For a given insulator region, if the surface area is increased by a factor *α,* consequently the current density *J* will be reduced by the same factor (*J*plain/*J*textured = α). Similarly, if a textured pattern increases the creepage distance by a factor *β*, the electric field strength will be reduced by the same factor as well (*E*plain/*E*textured = β) Given that power dissipation is related with *E* and *J* according to the relationship given by Equation (8), a textured pattern would reduce the surface power dissipation per unit area of the insulator surface *P* (Wim^{-2}) by a combined factor $\alpha \times \beta$:

$$\frac{P_{plain}}{P_{texteured}} = \frac{E_{plain} \times J_{plain}}{E_{texteured} \times J_{texteured}} = \alpha \times \beta \quad (7)$$

$$P = E \cdot J \quad (8)$$

While the well-established anti-fog designs increase only the creepage distance, thus affecting only factor β, textured patterns could control both the surface area (factor α) and the creepage distance (factor β) independently, thus achieving different combined power density factors $\alpha \times \beta$. This combined factor could function as a figure of merit for the ability of the textured design to inhibit the drying of the pollution layer by decreasing the surface power dissipation.

II.3.3. Theoretical classification of candidate textures

A theoretical classification of the candidate textures that would be assessed for the development of textured insulator prototypes was conducted based of the combined power density factor. Geometrical calculations on the patterns shown in Figure 2 are shown in Table 1.

Table II. 1. Theoretical classification of textured patterns. Table adopted from [14].

Texture	Area factor α	Creepage factor β	Power density factor αβ
1. Contiguous hexagonal	1.907	1.209	2.306
2. Intersecting hexagonal	1.446	2.356	3.407
3. Intersecting square	1.301	2.222	2.891
4. Intersecting triangular	1.209	1.814	2.193

The calculations presented in the above table suggested that based on the power density factor as a figure of merit for the anti-dry band performance, the contiguous hexagonal, the intersecting hexagonal and the intersecting square patterns were the most promising textures.

Early stage tests reported in [14] on non-textured silicone rubber samples and silicone rubber samples with a textured finish, similar to the contiguous configuration, showed some promising results. The present research work will describe the laboratory investigations of these textured patterns in a series of material tests and the development and testing of full textured insulators in clean-fog tests.

II.3.4. Extraction

The design and selection of outdoor insulators are significantly influenced by pollution contamination, which can lead to surface discharges and flashover events. Polymeric materials are commonly used to improve insulator performance due to their water repellent properties, but they

can suffer from ageing degradation. To address these issues, a research program is proposing textured insulator designs with hemispherical protuberances to reduce damage from surface discharges and enhance flashover performance. Experimental investigations are being conducted to assess the effectiveness of these textured insulators using standard and novel test methods and diagnostic tools.

II.4. Textured Polymeric Insulators for Application at 400 Kv

II.4.1. 400 kv insulator prototypes

Several key innovations have been developed for the process of design and manufacture of these textured insulators by Allied Insulators Ltd to allow superior and optimized performance. The main Manufacturing Challenges were:

- Seamless HTV Injection Moulding
- Preserving the intricate detail and geometry of textured surface
- Fully circumferential texturing without mould flash lines:
  - The textured surface must exhibit the same properties as the rest of the housing.
  - Moulded parts become trapped in the tooling hence a method was required to extract the textured shed without any separation of the mould plates.
  - Design of Triple point Interface
  - In order to preserve the integrity of the existing interface design special consideration required to accommodate the texturing.
  - Repeatable consistent manufacturing quality
  - Proven scalability, with the manufacturing problems solved its easy to upscale from the short prototypes to 400kV Insulators
  - Identical non-textured control insulators manufactured in both short prototype for laboratory tests and 400kV for NG outdoor test station

Rectangular samples and 400 kV insulators prototypes were fabricated exploiting the accumulated experience by AHIVEC research team. The manufactured flat samples with conventional smooth surfaces and textured surfaces were tested to obtain a comparative material test. The material is based on SiR with other fillers used for commercial outdoor polymeric insulators. The retained texture was patterns (C). Concerning the 400 kV insulators, two different insulators prototype were manufactured with two profiles: conventional (CONV) and textured (TXT). Besides the 400kV insulators, a first prototype insulators with 7 sheds only (7S) with regular sheds inclination, as presented in Figure 3-a, were manufactured. The geometrical parameters are given in [16].

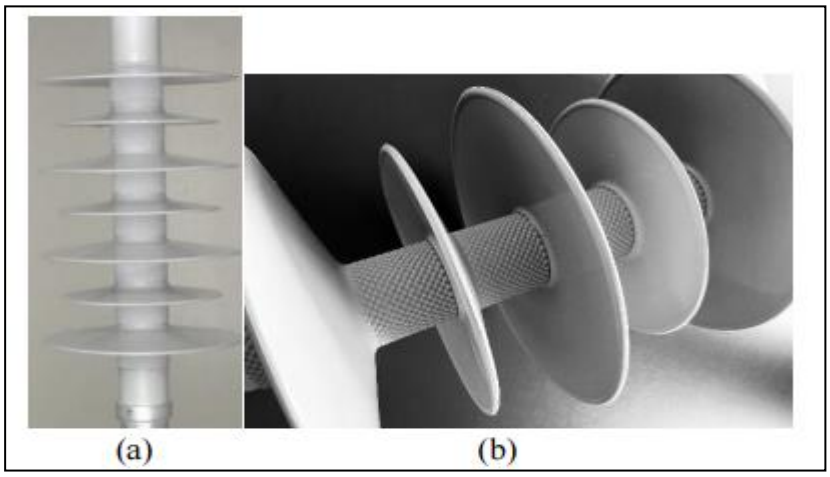

Figure II. 3. Manufactured samples for laboratory tests. (a): 7 sheds textured prototype, (b): 5 sheds textured modified and improved design prototype.

II.4.1.1. Inclined plane tests results

Inclined Plane Test according to the standard IEC 60587 [17] was applied to rectangular samples. The test sample dimensions were in accordance with IEC-60587 standard, 120mm x 50 mm x 6 mm. Test samples were fabricated with both conventional non-textured flat surfaces. All tha samples passed the test regarding the IPT current criterion (60 mA during 2 seconds). But some differences are observable and highlighted.

Figure 4-a shows the discharge behavior and temperature distribution during the test with conventional manufacturer's sample while Figure 4-b illustrates typical parallel streamers appearing on textured samples [18]. Figure 3 shows that, after a period of test time, the temperature activity is concentrated along the central path of the sample along the creepage distance. During the test, dry band arcs activity became more localized at the ground electrode where unstable metal-arc discharges tend to anchor at one location with a consequent increase of the temperature. In the case of TXT samples, the temperature is distributed across the insulator sample which increases the thermal dissipation. Figure 4 illustrates the rms average power during the test for both conventional and manufacturer's textured samples. Figure 7 shows the accumulated dissipated energy of the samples.

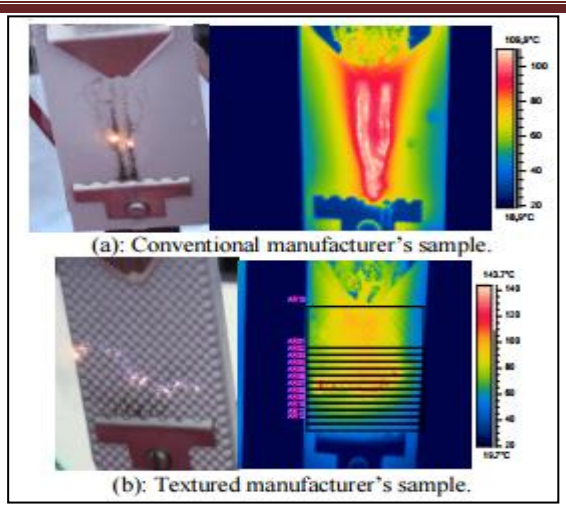

Figure II.4. Conventional and textured manufacturer's samples during an inclined-plane test [18].

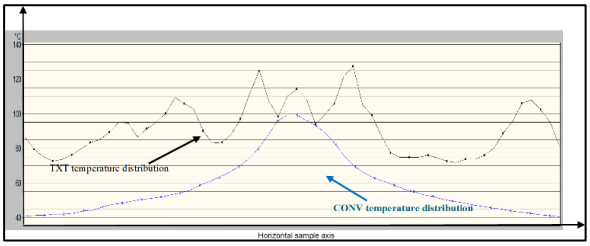

Figure II.5 . Distribution of the temperature along the insulation sample surface during inclined plane test.

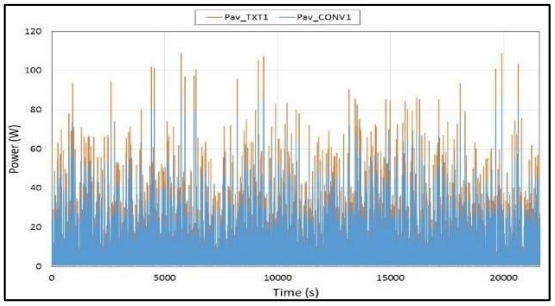

Figure II.6. Average power in inclined plane tests for materials used in manufactured insulators.

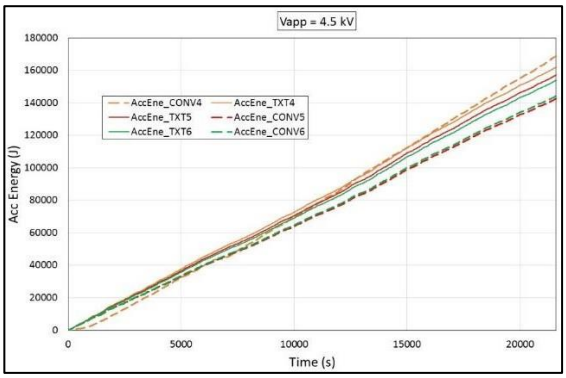

Figure II.7. Dissipated energy in inclined plane tests.

Table 2 illustrates the maximum tracking path, the superficialerosion path of the samples after 6 hours testing with different voltages (3.5 kV and 4.5 kV). No deep erosion path was observed or

exaggerate long tracking path for both profiles. Thetextured profiles showed better behavior where both of erosionand tracking paths are lower than for the conventional samples.

Table II.2. Maximum tracking and Superficial Max Erosion paths of tested samples after 6 hours IPT.

Sample pattern	Max Tracking Path (cm)	Superficial Max Erosion Path (cm)	Applied Voltage (kV)
TXT-1	3	0.8	3.5
TXT-2	3.6	0.9	3.5
TXT-3	3.6	0.7	3.5
TXT-1	3.5	0.9	4.5
TXT-2	1	0.5	4.5
TXT-3	4	0.6	4.5
CONV-1	5	1.2	3.5
CONV-2	4.4	1.4	3.5
CONV-3	4.7	2	3.5
CONV-4	4.9	2.1	4.5
CONV-5	4.7	3	4.5
CONV-6	5	2.9	4.5

PCM analysis showed also that apart from Silicone, Oxygen, Aluminum and Carbon,

Iron is present. The iron is the result ofthe metallic corrosion of the HV electrode. Also, some mineralslike Sodium, Calcium and Chloride. Few quantities of Sulphateand Manganese are also present because the contaminated flow.

The IPT showed that the used material is suitable for texturedprofile and presents resistance to electrical arc erosion.

II.4.1.2. Electrical parameters, thermal monitoring, and flashover under clean fog test

The adopted experimental setup and test procedure for evaluating and the comparison of the performance of both textured and conventional insulator sections are the same as presented in [16] and are based on standard IEC 60507 [19]. The pollution constitution consists of sodium chloride, 40 g/l of kaolin, wetting agent (Triton) and deionized water. The conductivity of the mixture depends on its sodium chloride content. Table 3 shows the used conductivities and their corresponding pollution level. The insulators are pre- conditioned with kaolin according to the CIGRE recommendation [20] before the application of the pollution.

Table II. 2. Adopted conductivity values.

Conductivity (mS/cm)	Pollution level
1.40	Light
3.50	Medium
8.60	Heavy
12.5	Severe

A. Prototype 7 sheds: 7S-CONV & 7S-TXT

The behavior of insulators depends on the profile of the insulator: textured insulators exhibit lower leakage current density (LC) and partial discharge activity compared to conventional insulators, regardless of pollution levels. Dry bands on textured insulators are more regular and mainly located in sleeve sections. Additionally, the accumulated dissipated energy (ADE) of textured insulators is lower than that of conventional insulators, which can be attributed to the increased heat dissipation efficiency of textures. To minimize discharge activity, a second prototype insulator with an improved design was manufactured, including textures covering the entire central part, increased shed inclination, and the addition of a "drip edge".

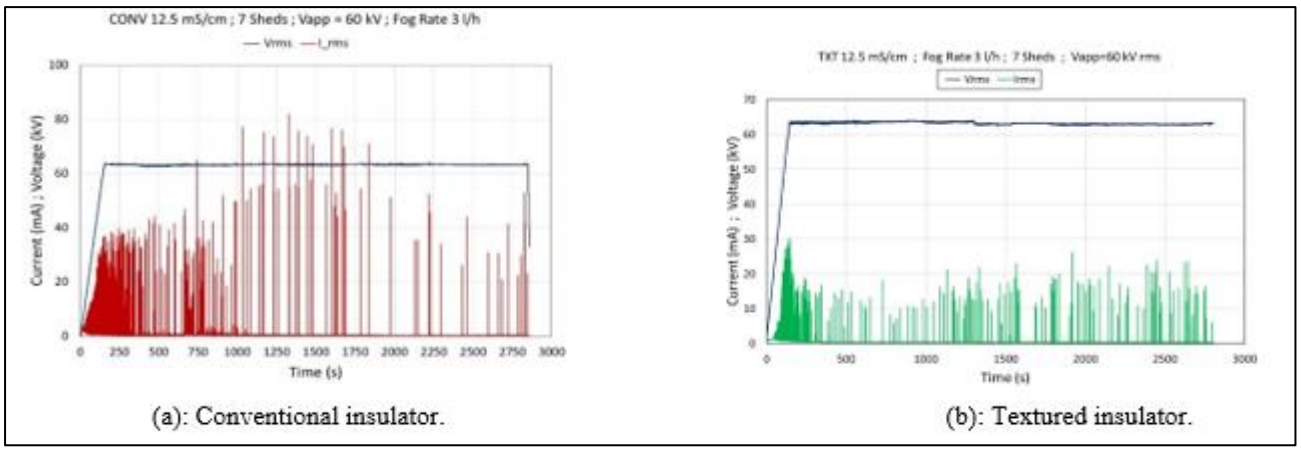

Figure II. 8. Leakage current of 7 sheds insulator with 60 kVrms applied voltage and severe pollution for both insulator profiles.

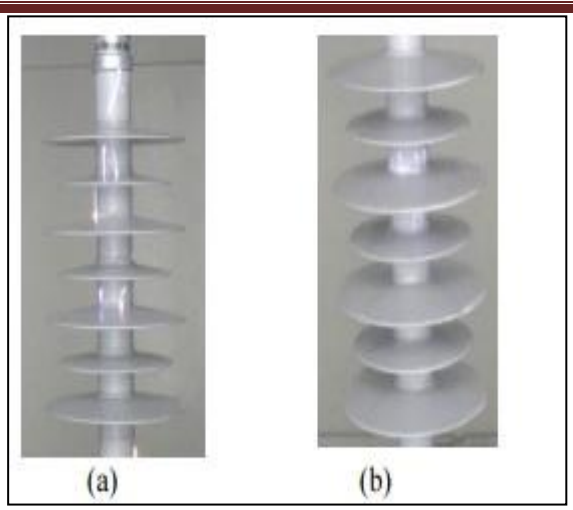

Figure II.9. Discharge activity on 7 shed insulators
(V= 60 kV rms, severe pollution).

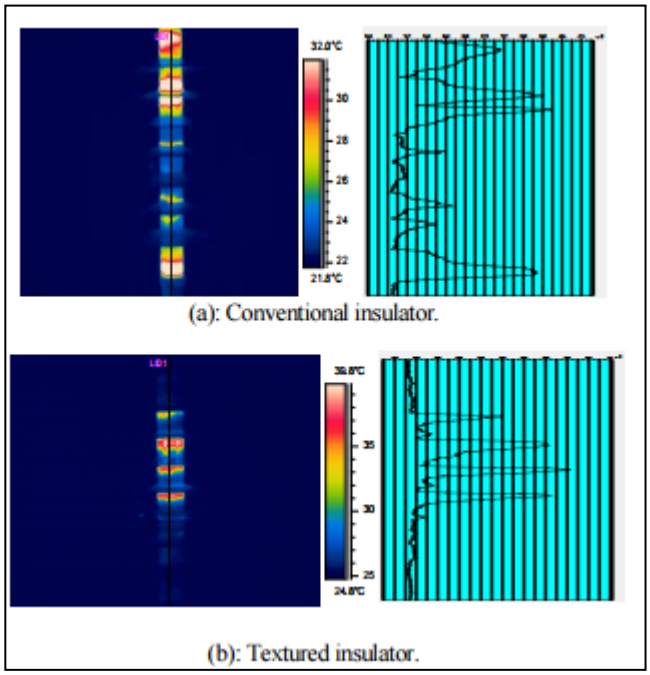

Figure II.10. Infra-red camera recording with severe pollution for both insulators and 60 kVrms applied voltage.

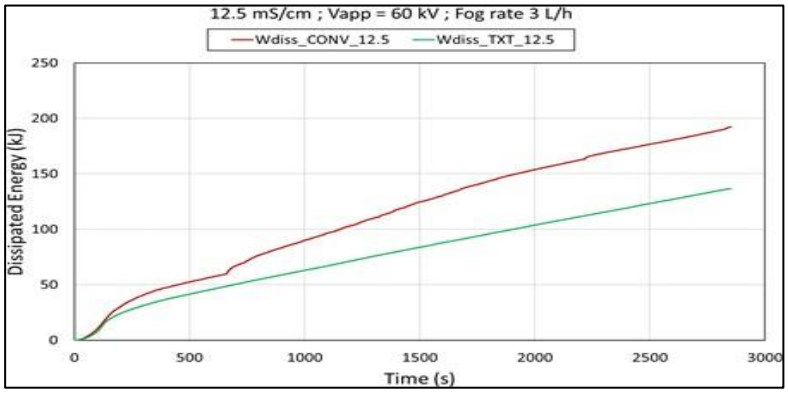

Figure II. 11. Comparative dissipated energy for 7 sheds insulators with both profiles: conventional and textured.

B. Prototype 5 sheds: 5S-CONV & 5S-TXT

The previous tests with 7 sheds insulators showed that the LC decreases with test duration. So, to avoid this disadvantage, different voltage levels were applied to the same 5 sheds insulator with shorter duration (an average of 10 minutes per voltage level). As for 7 sheds insulators, the LC behavior depends on the used insulator profile: 5S-TXT insulators LC isalways lower than 5S-CONV insulators LC whatever the pollution level. Figure 12 illustrates an example of the LC monitoring with different applied voltages for severe pollution.Regarding the ADE, the experimental results showed that 5S-TXT insulators exhibit lower ADE than 5S-CONV insulators as presented in Figure 13.

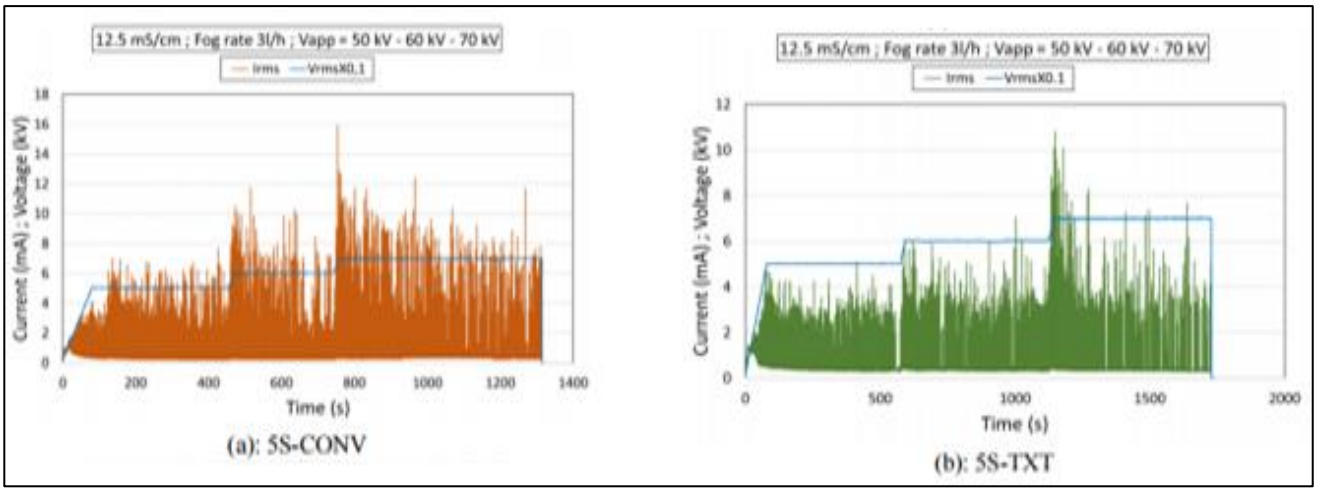

Figure II.12. Leakage current with multiple applied voltage levels and severe pollution with 5 sheds. (a): conventional, (b): textured.

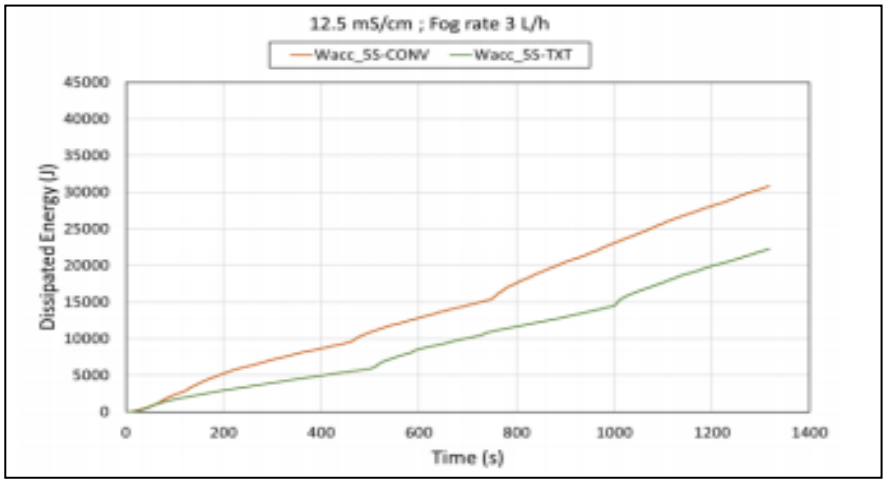

Figure II.13. Comparative dissipated energy for 5 sheds insulators with both profiles: conventional and textured.

Figure 14 demonstrates how the number of LC pulses varies across different normalized LC ranges and pollution levels for various insulators. Generally, as the LC range increases, the number of LC pulses decreases, especially in heavy and severe pollution levels. This decrease is attributed to the heightened

thermal effect with larger LC magnitudes, leading to fewer Dry Bands Discharges (dBs) and Dry Band Arcs (DBAs).The magnitude of LC pulses depends on the balance between re-wetting and thermal effects, influenced by pollution level s. Additionally, insulators with textured profiles show fewer LC pulses due to their enhanced ability to dissipate joule heating and create more challenging discharge paths.

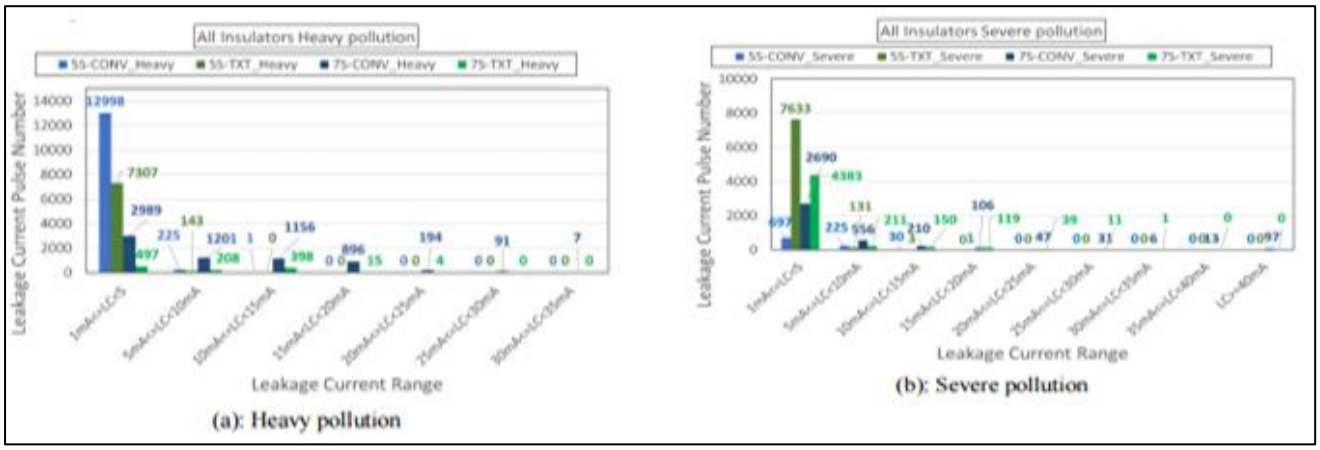

Figure II.14. Leakage current pulses number of both profiles and sheds design.

For flashover (FOV) tests, all the insulators have been tested with 3 sheds as illustrated in Figure 15. The procedure isthe same as described in the standard IEC 60-507 [19]. Steady fog with 3 litre/hour was applied, and the insulator is energizedwith low voltage (850 V) until the leakage resistance settles at the minimum value. At this point, a rise voltage ramp is applieduntil FOV occurs. A series of 10 FOV tests were applied to eachinsulator and the average FOV voltage are illustrated in Figure 15.

The results show that textured profile exhibits better performance FOV tests than CONV profile whatever the used insulator profile (7S or 5S). These results are in accordance withthe results of AHIVEC manufactured insulators. On the other hand, FOV tests confirm the superiority of the 5S prototype compared to the 7S prototype both insulator design profiles (TXT or CONV).

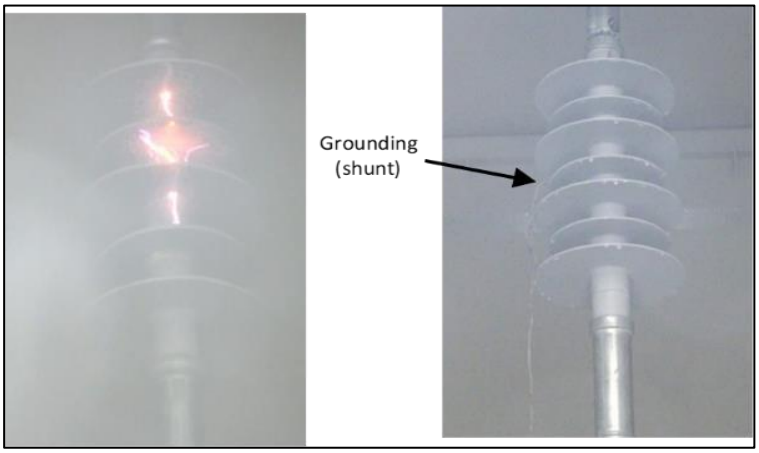

Figure II.15. Insulator configuration setup for pollution flashover test. (a): pre-flashover, (b): insulator grounded at the 3rd shed.

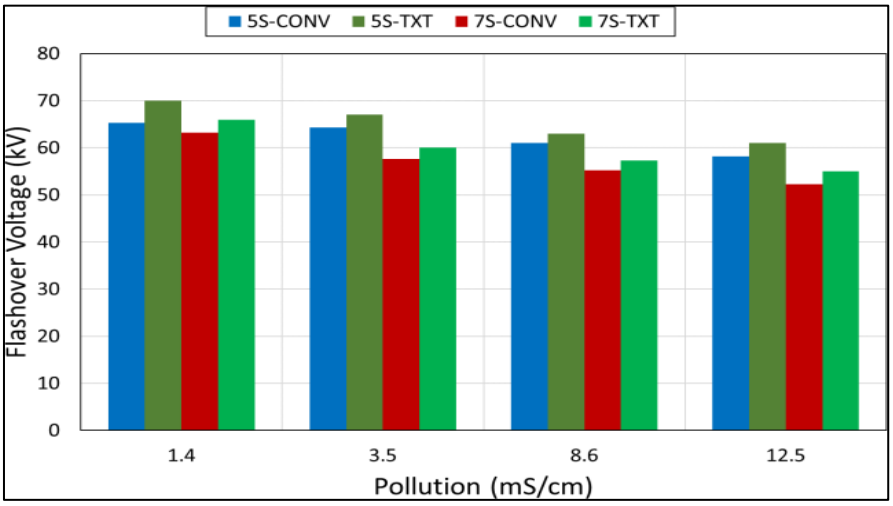

Figure II.16. Average flashover voltages of all the insulators for different pollution levels.

C. Deeside Natural Pollution Monitoring Station

A collaborative research project was developed with National Grid Electricity Transmission -UK for testing and monitoring energized 400 kV textured and conventional insulators in natural environment. For that purpose, a pollution monitoring station was designed and proposed by the AHIVECteam and is mainly constituted by:

LC monitoring system: peak, surge counting, charges,power loss, harmonics, power factor index and cumulative energy.

- ESDD/NSDD measurement.
- Pollution index.
- Weather and UV-B monitoring.
- Thermal camera monitoring.
- Corona-UV monitoring and visual camera monitoring.

Six 400 kV insulators string were installed as presented in Figure 17: 3 textured and 3 conventional. The insulators are energized with 230 kV (phase-ground) via a transformer. Figure 18 shows 2D and 3D drawing of the tested textured insulators.

Figure II.17. Tested 400 kV insulators at Deeside station (National Grid, Deeside Centre for Innovation).

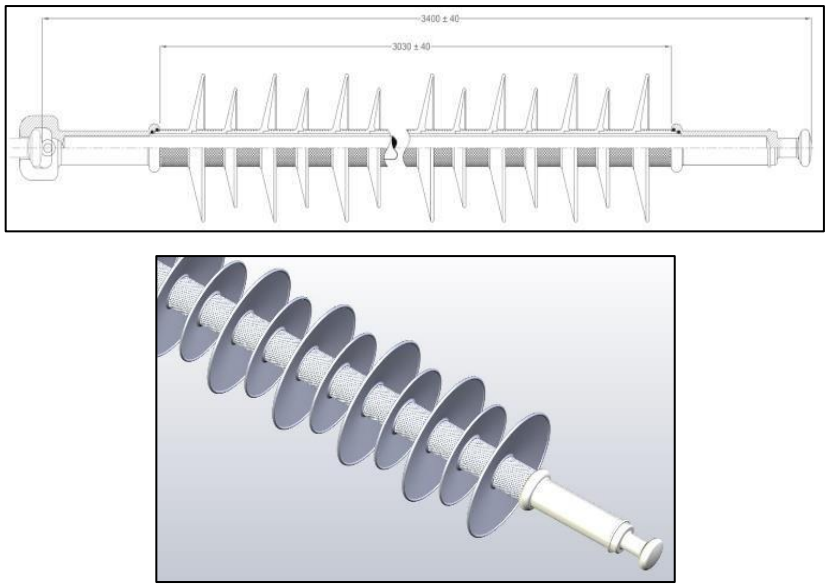

Figure II. 18. Drawing of 400 kV textured insulator tested at Deeside station.

✓ **Extraction**

This study presents recent advancements in the development of textured insulators for high-voltage electrical networks. Tests have shown that textured insulators outperform conventional ones in terms of leakage current and thermal performance, regardless of the prototype configuration. Additionally, insulators with 5 sheds exhibit better performance than those with 7 sheds, with a higher flashover breakdown voltage. The results underscore the importance of profile and prototype in managing leakage current. A natural pollution monitoring station has been set up to continue research in the future.

II.5. Conclusion

In conclusion, the use of textured insulator surfaces with hemispherical protuberances represents a promising approach to improving the pollution performance of outdoor insulation systems, particularly in polymeric insulators. These textures, leveraging silicone rubber's molding properties, aim to reduce the damaging effects of surface discharges by improving dry banding distribution and flashover performance. Collaborative efforts between industry and research institutions have led to successful laboratory testing, demonstrating superior performance compared to traditional insulators. Ongoing field trials on transmission systems up to 400 kV will provide further validation of these textured insulators' effectiveness in real-world conditions. Overall, this technology offers a potential

solution to enhance the reliability and performance of outdoor insulation systems, with further research and testing needed for broader implementation in power transmission networks.

CHAPTER III:

EXPERIMENTAL STUDY AND RESULTS

III.1. Introduction

A recently proposed design for polymer insulators, consisting of a series of semi-elliptical protrusions, aims to reduce energy dissipation by decreasing both the electric field (E) and leakage current density (J), while increasing the longitudinal leakage path without increasing the total length of the insulator. Additionally, the formation of parallel current paths can lead to less harmful discharges. Initial reports have shown that introducing such a surface texture results in improved performance compared to conventional samples with smooth surfaces.

Materials intended for use in external insulation should be tested for their ability to resist abrasion and surface tracking. The inclined plane test is an accelerated aging test in which rectangular specimens are subjected to high electrical stresses to study material performance against corrosion and surface tracking. In this chapter, we will study experiments on three samples made of plastique (PLA+) using a non- textile surface, a transversely textile surface, and a longitudinally textile surface for comparison.

III.2. Experimental Setup

III.2.1. High Voltage Laboratory Test Circuit (University of El Oued)

The tests are conducted in the high voltage laboratory at the University of El Oued.

Our laboratory is equipped with three voltage sources:

- A power supply with an industrial frequency of 50Hz.
- A DC voltage generator.
- An impulse voltage generator.

III.2.1.1. Test Station Equipment

The test station in our laboratory comprises the following components:

- A test transformer.
- A regulating transformer.
- Voltage dividers.
- A control panel with measuring and protective devices.
- A digital oscilloscope.
- Conductivity measuring device.

III.2.1.2. Test Transformer

We used a test transformer designed and insulated for high-voltage generation. It has a transformation ratio of 250V/100kV, with a power rating of 5 kVA. This transformer allows the high voltage at the secondary side to be varied from 0 to full voltage.

III.2.1.3. Regulating Transformer

We allow for the variation of the voltage at the terminals of the test transformer. Its transformation ratio is 220V/250V.

III.2.1.4. Digital Oscilloscope

It is a device that allows for the visualization of waveforms and recorded phenomena (Figure III.1).

Figure III.1. Digital Oscilloscope.

III.2.1.5. Control Panel

This panel is powered by a 220V supply. It allows for the automatic variation of the test voltage. See Figure (III.2).

Figure III.2. Photo of the control panel in the high voltage laboratory at the University of El Oued.

III.2.1.6. Measurement and Protection Devices

The laboratory power supply is controlled from a control panel located in the laboratoryoutside the test platform (the Faraday cage). The high-voltage transformer and its regulator are independently protected by a 250A fuse and a thermal relay. These protections are connected to the main contactor coil circuit, providing sufficient protection against transformer overloads and short-circuit currents.

For voltage measurements, we have:

- DSM: a digital voltmeter for measuring alternating voltage.
- DGM: a digital voltmeter for measuring direct voltage.
- A voltmeter and ammeter for measuring primary voltage at the test transformer.

III.2.1.7. Voltage Divider

There are two types of voltage dividers:

- A capacitive voltage divider for measuring industrial frequency voltage.
- A resistive voltage divider for measuring DC voltage.

III.2.1.8. Alternating Voltage Test Circuit

High-voltage alternating current generators, operating at frequencies between a few Hz and 1 kHz, generally use step-up transformers.

High-voltage alternating current generators are used for:

- High-voltage alternating current tests (high-voltage transformers).
- Power supply (high-voltage transformers) for DC rectifiers, oscillating circuit generators, and impulse generators.

Figure III.3 shows the alternating voltage test circuit realized in the high-voltage laboratory, and Figure III.4 is a corresponding photo of the setup in the high-voltage laboratory.

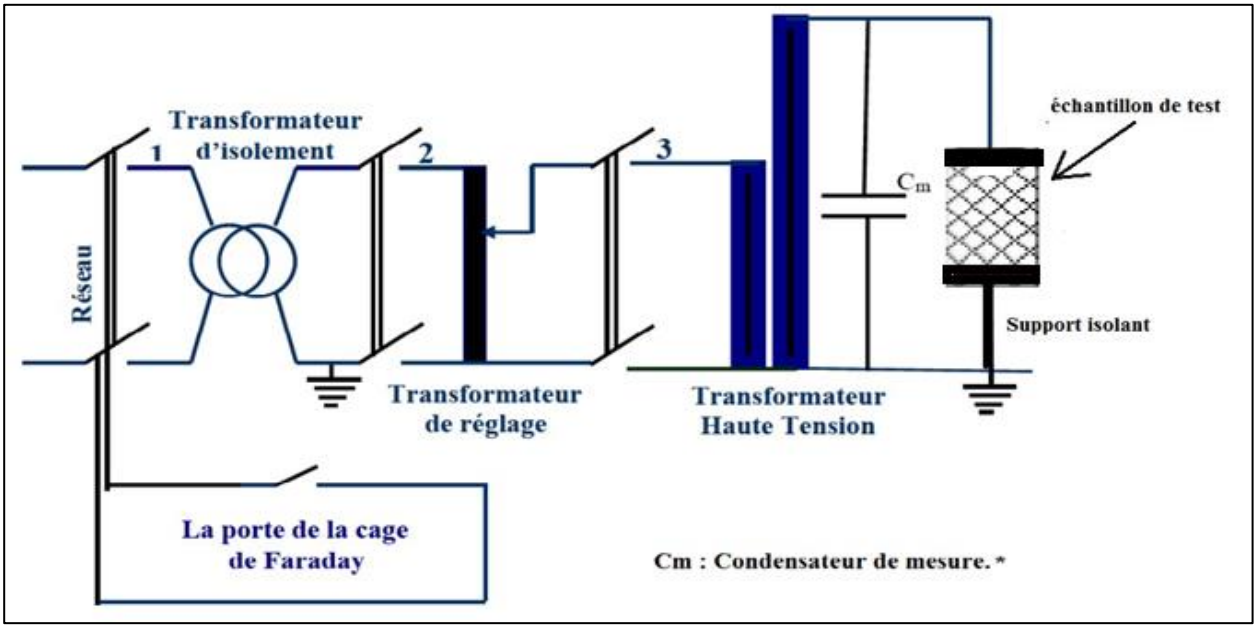

Figure III.3. Industrial Frequency Test Circuit.

Figure III. 4. Photo of the Industrial Frequency Test Circuit.

III.3. Operating mode

Most studies consider experimental models of simple geometry and rarely the profile of a real insulator. However, while these equivalent models do not exactly reflect the behavior of real insulators, they allow for a better visualization of the electrical discharge phenomenon.

III.3.1. Experimental model

Rectangular PLA^{+} samples were made. The dimensions were 120 mm x 48 mm x 5 mm. Two samples were prepared, a conventional non- textured sample and a textured sample. The lengths and widths of the samples are indicated in Figure 5.

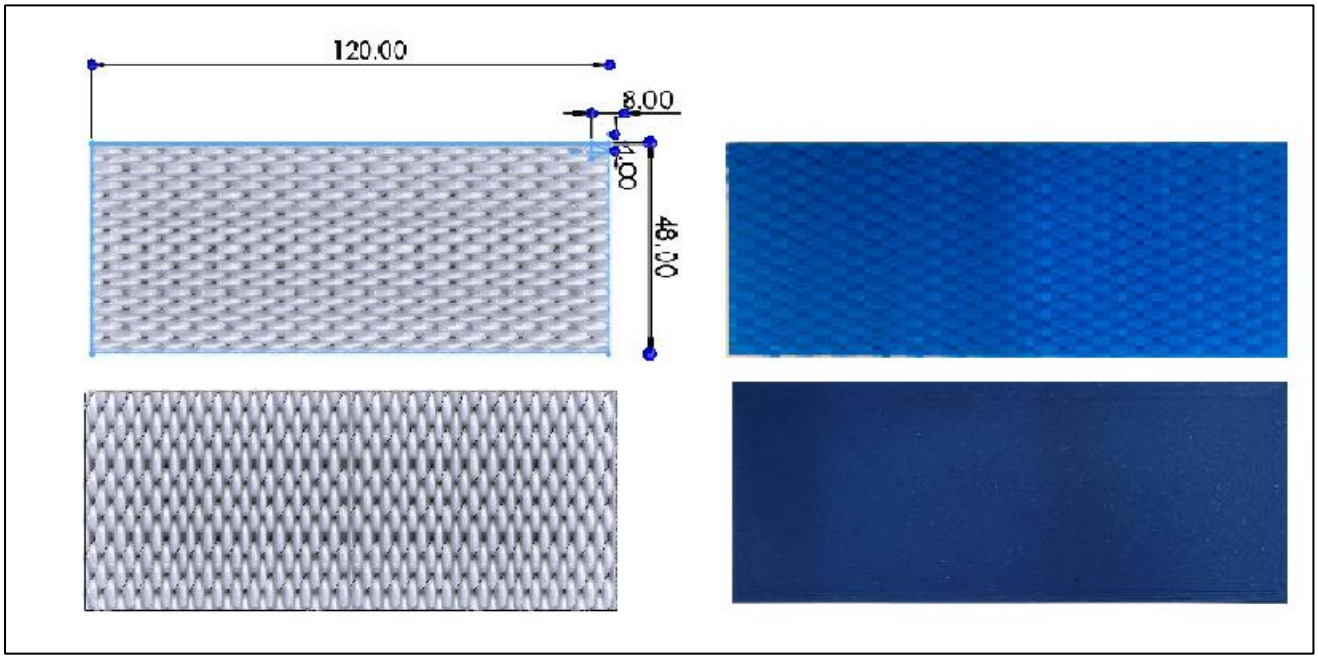

Figure III.5. Two samples : a traditional non- textured sample and a woven sample, along with their dimensions.

III.3.2. Preparation of the model

Before each series of tests, the insulating panel is carefully cleaned and then soaked in gas oil in the areas where the galvanized steel electrodes will be placed to ensure close contact between the panel and the electrodes without leaving any gaps. The panel is then wiped with cotton soaked in alcohol to remove any residue of gas oil from the insulating surface. We then installed aluminum foil on the insulator as electrodes, changing the distance between them to 2 cm, 4 cm, 6 cm, 8 cm, and finally 10 cm in all three cases: non- textured, textured transversely, and textured longitudinally.

III.4. Test Procedure

The objective of these tests is to study how the leakage current and the flashover voltage evolve based on the applied electro-geometric parameters on the laboratory model.

III.4.1. Flashover Voltage Measurement

The determination of the flashover voltage (representing the arithmetic mean of three values) from the two samples. These measurements determine the limit voltage levels that will be applied to measure the leakage current.

III.4.2. Leakage Current Measurement

For different levels ranging from 5 kV to 20 kV in steps of 5 kV, and for each configuration, the amplitude of the leakage current is determined by measuring the voltage across a non-inductive 10 KΩ resistor inserted in the earth return. For this, we used a memory oscilloscope with a bandwidth of 25 MHz. To avoid any influence of noise in the captured signal, we place the resistor in an aluminum metal box grounded, thus forming an electrostatic shield.

III.4.3. Atmospheric Correction

For each test conducted, the atmospheric conditions are recorded using a special electronic device, as shown in Figure III-6.

Figure III.6. Measurement instrument for atmospheric conditions (humidity, temperature, and pressure).

III.4.4. Influence of Air Relative Density

Temperature and pressure influence the dielectric strength of air. In IEC 60 (International Electrotechnical Commission), we find the concept of relative density, which is defined as the ratio of the density of air under given pressure (P) and temperature (T) conditions to the density of air under standard atmospheric conditions, i.e.:

- Ambient temperature T0 = 28°C.

- Atmospheric pressure P0 = 1008 mbar (= 756 mm Hg).

$$\partial = \frac{293}{760} * \frac{P}{(273+T)} \quad (1)$$

∂ is the correction factor for air density.

The pressure P is in mbar and the temperature T is in °C.

This equation is used to convert the measured discharge voltage Um under test atmospheric conditions (temperature T and pressure P) to the value Ucr that would have been obtained under standard conditions (T0 and P0):

$$\mathbf{Ucr} = \frac{\boldsymbol{Um}}{\boldsymbol{\partial}} \leq \mathbf{1}$$

III.4.5. Influence of Humidity

In the case of fast or very fast waves, such as those caused by lightning, the breakdown voltage is less sensitive to humidity variations. Therefore, during our tests, where the relative humidity varied between 34% and 56%, we did not take this aspect into account.

III.5. Experimental Results

Below, we examine the effect of textured and non- textured samples on the behavior of the laboratory model. The experimental results focus on the changes in voltage and leakage current. A set of parameters were applied to the experimental model.

III.5.1. The non- textured sample

The following table represents the variations in flashover voltage and the effect of corona and partial discharge in the case of the non- textured sample with adjustment of the distance between the electrodes. Additionally, it includes selected real images during the experiment.

Table III.1. The table represent changes in voltage across the non- textured sample at varying dimension between the electrodes.

		1	2	3	Average	Corrected
The dimension between the electrodes is 4 cm	Corona effect	15.50	15.86	14.86	15.40	17.11
	Partial discharge	28.15	27.14	28.12	27.80	30.88
	Flashover voltage	34.61	34.50	34.20	34.43	38.25
The dimension between the electrodes is 8 cm	Corona effect	29.35	30.00	31.21	30.18	33.54
	Partial discharge	48.60	48.75	49.10	48.81	54.24
	Flashover voltage	57.54	57.60	58.31	57.81	64.24

Figure III .7. Real images of the flashover voltage variation in the non- textured sample at different dimension between the electrodes : (A) 4cm, (B) 8 cm.

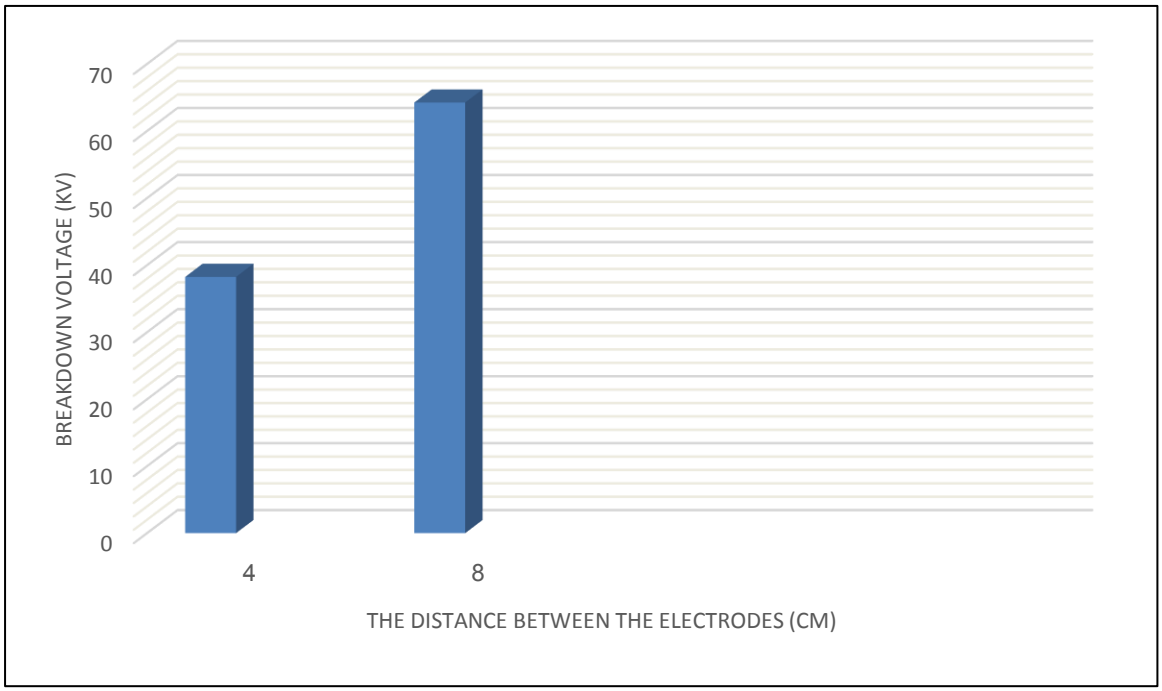

Figure III. 8. Graph showing the change in flashover voltage in the non- textured sample.

III.5.2. Longitudinally Textured Sample

The following table represents the variations in flashover voltage and the effect of corona and partial discharge in the case of the Longitudinally textured sample with adjustment of the distance between the electrodes. Additionally, it includes selected real images during the experiment.

Table III.2. The table represent changes in voltage across Longitudinally Textured Sample at varying dimension between the electrodes.

		1	2	3	Average	Corrected
The dimension between the electrodes is 4 cm	Corona effect	16.68	18.55	20.45	18.56	20.64
	Partial discharge	31.61	31.64	31.56	31.60	35.11
	Flashover voltage	38.65	35.34	36.96	36.98	41.08
The dimension between the electrodes is 8 cm	Corona effect	24.20	25.10	25.25	24.85	27.61
	Partial discharge	55.14	56.12	55.14	55.46	61.62
	Flashover voltage	64.85	65.19	64.18	64.73	71.92

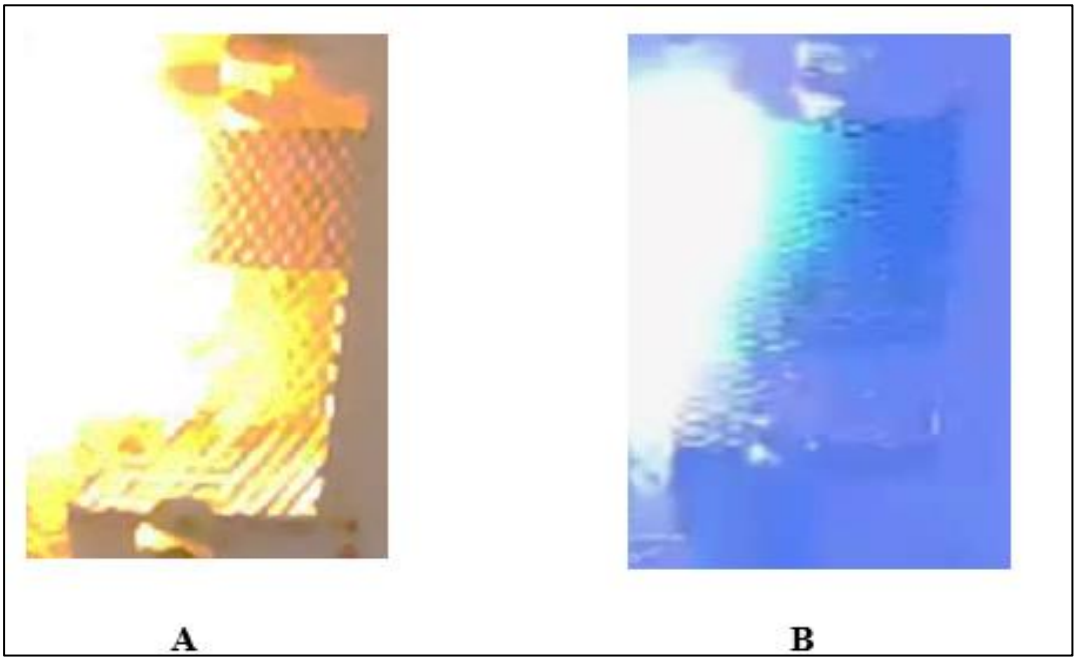

Figure III. 9. Real images of the flashover voltage variation in the Longitudinally textured sample at different dimension between the electrodes : (A) 4cm, (B) 8 cm.

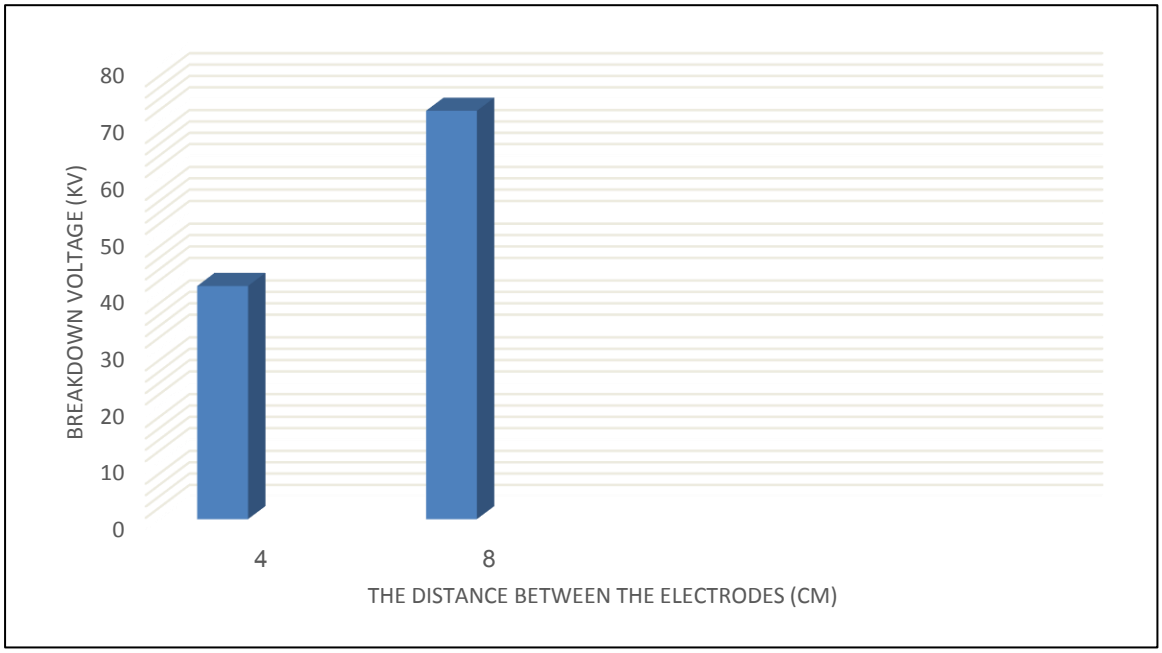

Figure III.10. Graph showing the change in flashover voltage in the Longitudinally textured sample.

III.5.3. Transversely Textured Sample

The following table represents the variations in flashover voltage and the effect of corona and partial discharge in the case of the Transversely textured sample with adjustment of the distance between the electrodes. Additionally, it includes selected real images during the experiment.

Table III.3. The table represent changes in voltage across Transversely Textured Sample at varying dimension between the electrodes.

		1	2	3	Average	Corrected
The dimension between the electrodes is 4 cm	Corona effect	22.86	23.41	22.50	22.92	25.46
	Partial discharge	32.02	32.51	32.87	32.46	36.06
	Flashover voltage	36.22	36.55	36.87	36.54	40.60
The dimension between the electrodes is 8 cm	Corona effect	27.56	29.36	28.41	28.44	31.60
	Partial discharge	47.75	48.88	49.16	48.59	53.98
	Flashover voltage	62.41	61.53	63.37	62.43	69.41

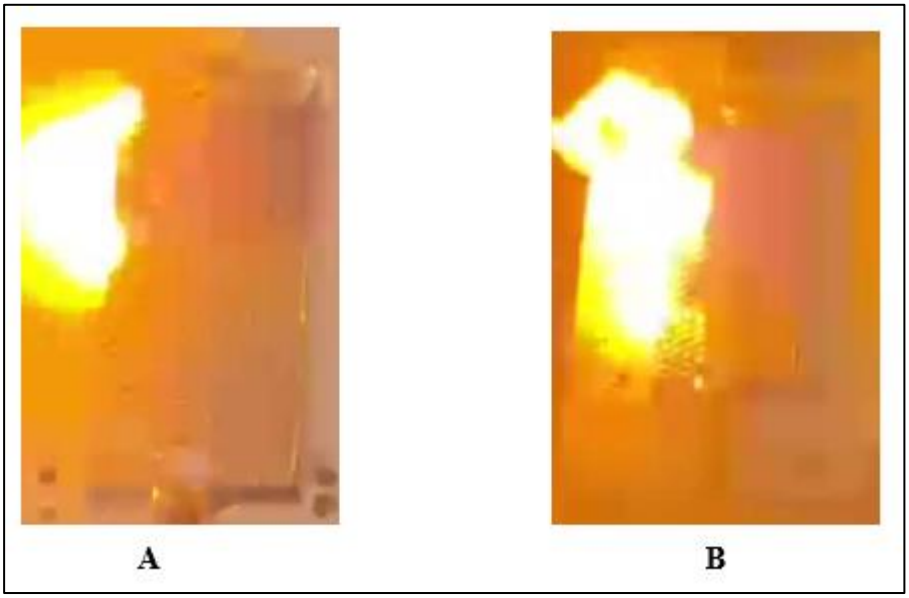

Figure III.11. Real images of the flashover voltage variation in the Transversely textured sample at different dimension between the electrodes : (A) 4cm, (B) 8 cm.

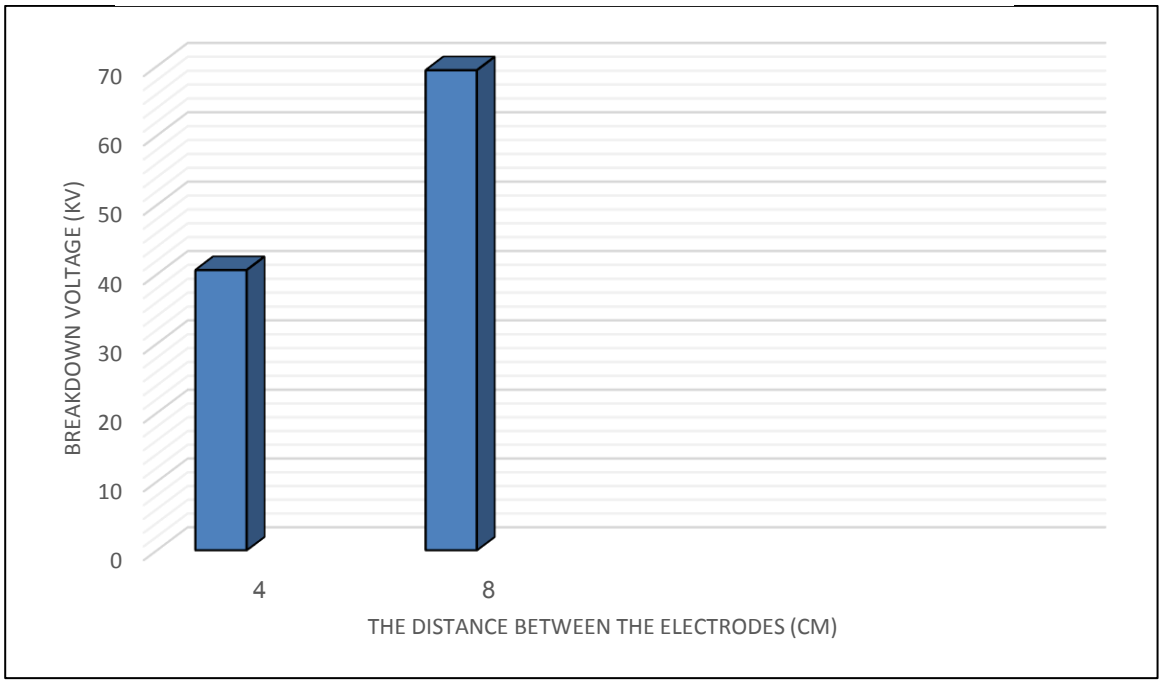

Figure III.12. Graph showing the change in flashover voltage in the Transversely textured sample.

III.5.4. Comparison of the three different cases

Based on the provided data, I can make the following comparisons between the three different surface textures (non-textured, longitudinally textured, and transversely textured) for the flashover voltage:

- At both electrode distances (4 cm and 8 cm), the non-textured sample exhibited the lowest flashover voltage among the three surface textures.

- At 4 cm distance, the longitudinally textured sample had the highest flashover voltage, while at 8 cm distance, the transversely textured sample had the highest flashover voltage.

In summary, the Longitudinally textured sample generally exhibited the highest flashover voltage, among the three surface textures, indicating better insulation performance under the inclined plane test conditions. The non-textured sample consistently showed the lowest values for these parameters, suggesting poorer insulation performance compared to the textured samples. And this is illustrated in the graph.

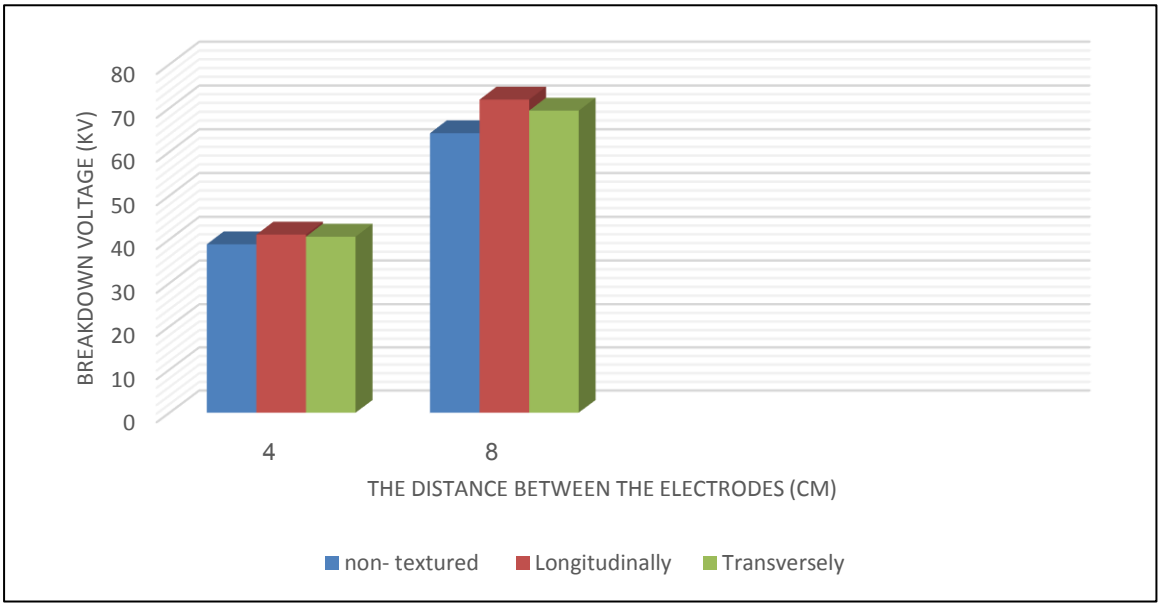

Figure III.13. Graph illustrates the variation in flashover voltage in the three samples.

III.5.5. Leakage current

Here we are studying the effect of samples on the value of leakage current. Therefore, different voltage levels and distances were considered.

$$\mathbf{I} = \frac{\mathbf{U}}{\mathbf{R}} \quad / \quad R = 10\ K\Omega$$

III.5.5.1. The non- textured sample

Table III.4. The table represents the values of current leakage at different voltages

Voltage (KV)	The dimension between the electrodes is 4 cm	The dimension between the electrodes is 8 cm
	The current leakage value at different voltages(µA)	
2	10.01	8.90
5	12.20	10.90
8	19.20	15

- The dimension between the electrodes is 4 cm

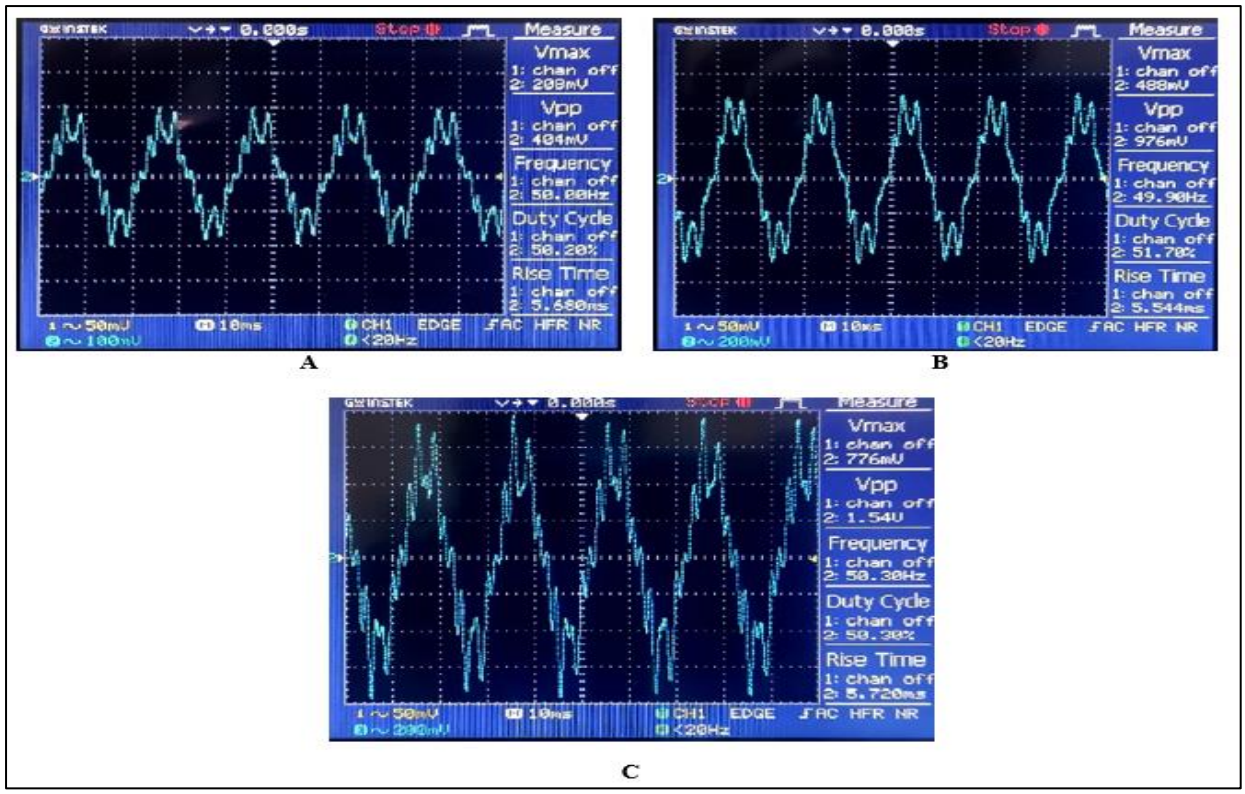

Figure III.14. Graphical curves of leakage current for the non- textured sample under different voltages: (A) 2KV, (B) 5KV, (C) 8KV.

- The dimension between the electrodes is 8 cm**Figure**

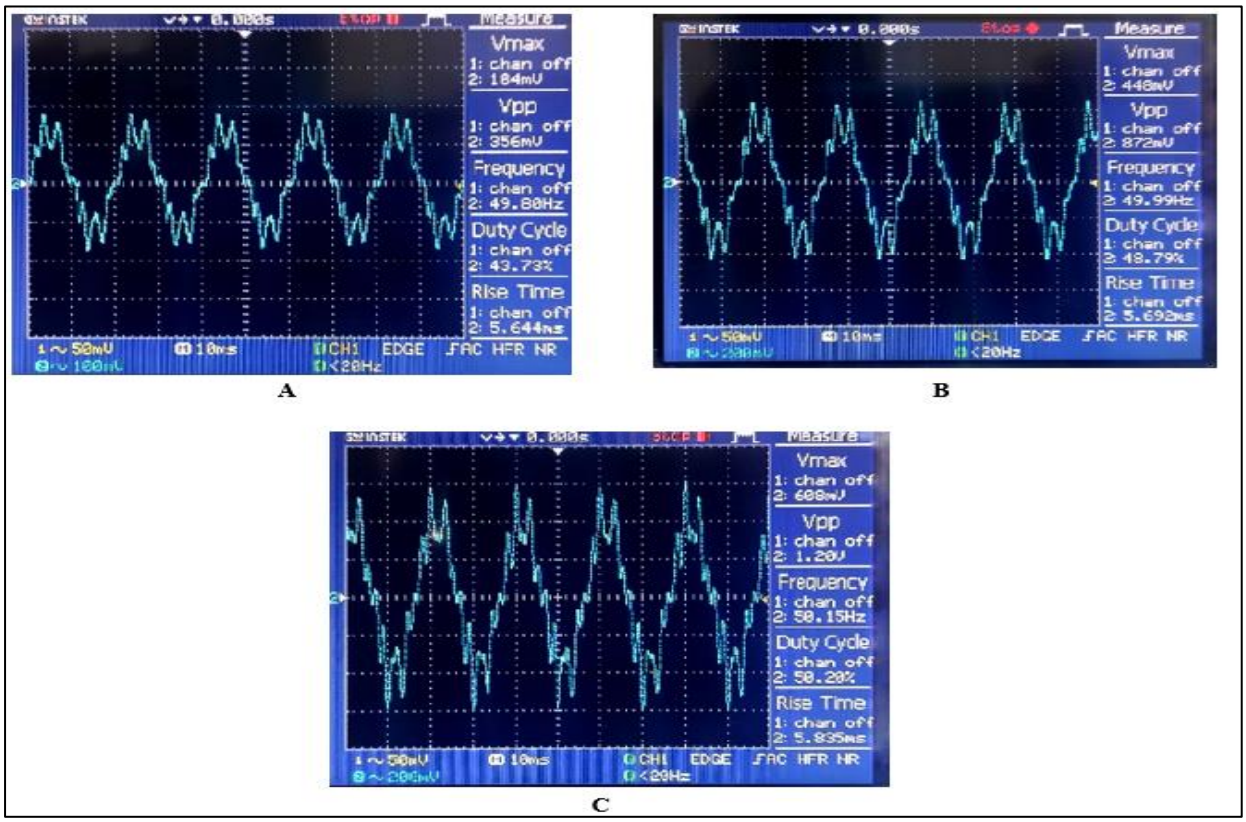

Figure III.15. Graphical curves of leakage current for the non- textured sample under different voltages: (A) 2KV, (B) 5KV, (C) 8KV.

III.5.5.2. Longitudinally Textured Sample

Table III.5. The table represents the values of current leakage at different voltages

Voltage (KV)	The dimension between the electrodes is 4 cm	The dimension between the electrodes is 8 cm
	The current leakage value at different voltages(µA)	
2	1.20	1
5	2.80	2.20
8	4	3.20

- <u>The dimension between the electrodes is 4 cm</u>

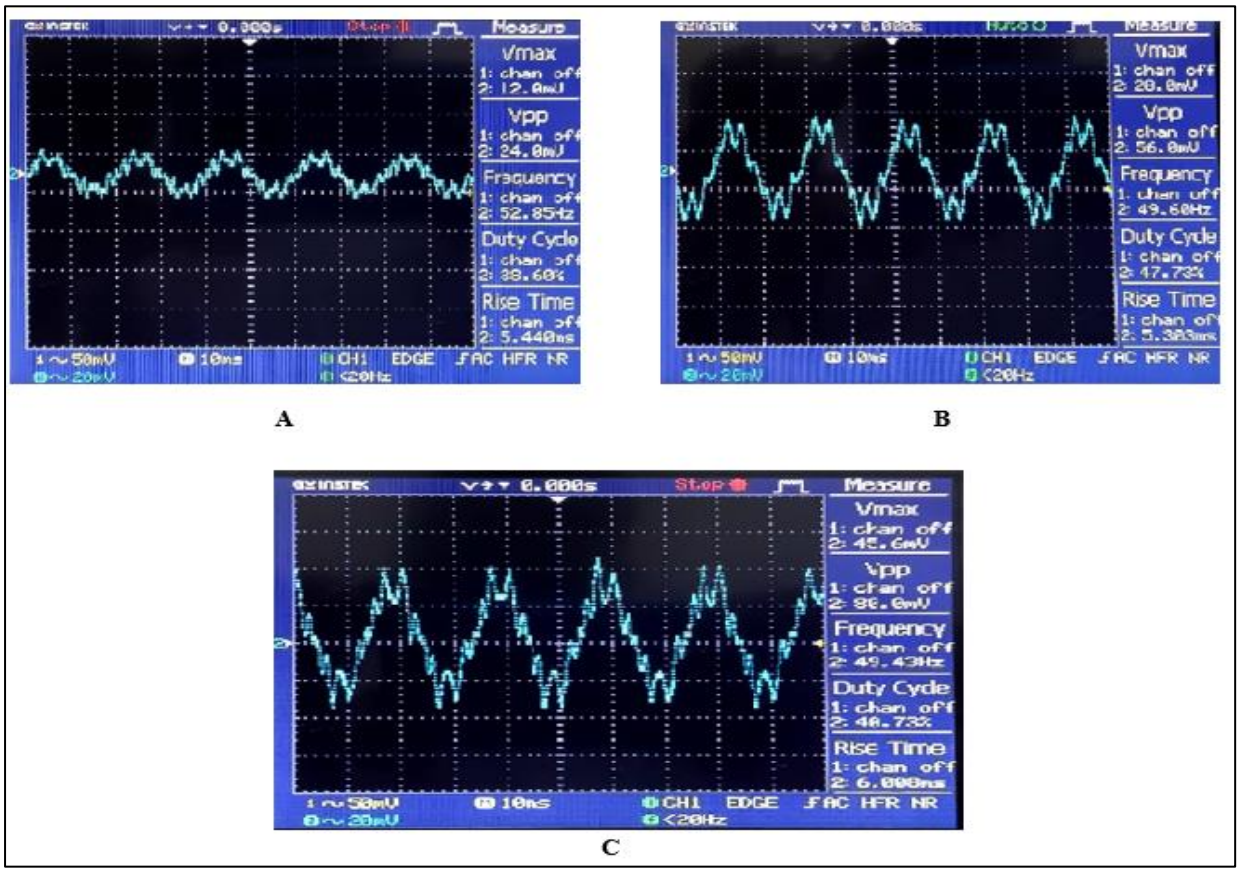

Figure III. 16. Graphical curves of leakage current for the Longitudinally textured sample under different voltages: (A) 2KV, (B) 5KV, (C) 8KV.

- The dimension between the electrodes is 8 cm

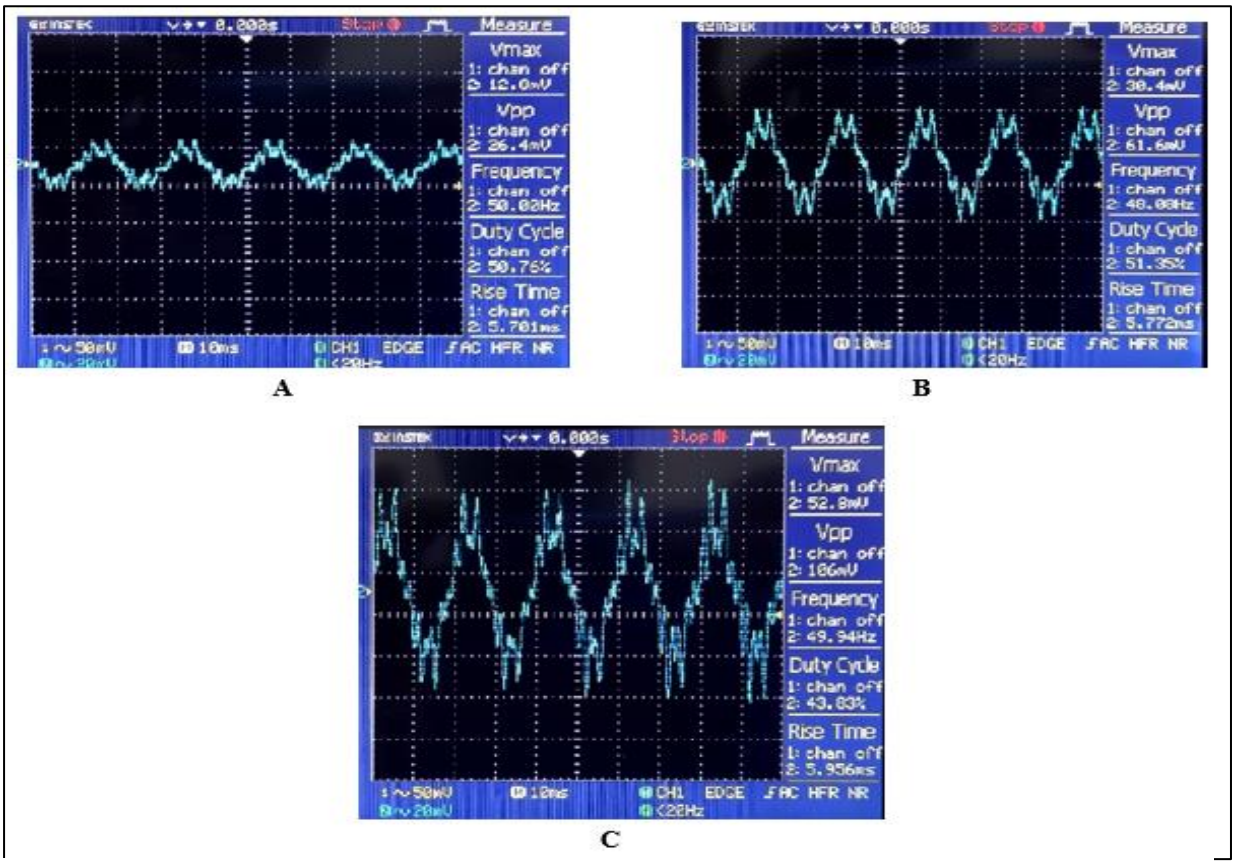

Figure III.17. Graphical curves of leakage current for the Longitudinally textured sample under different voltages: (A) 2KV, (B) 5KV, (C) 8KV.

III.5.5.3. Transversely Textured Sample

Table III.6. Table III.6. The table represents the values of current leakage at different voltages

Voltage (KV)	The dimension between the electrodes is 4 cm	The dimension between the electrodes is 8 cm
	The current leakage value at different voltages(µA)	
2	1.20	1.10
5	3.08	2.40
8	5.30	4.50

- The dimension between the electrodes is 4 cm

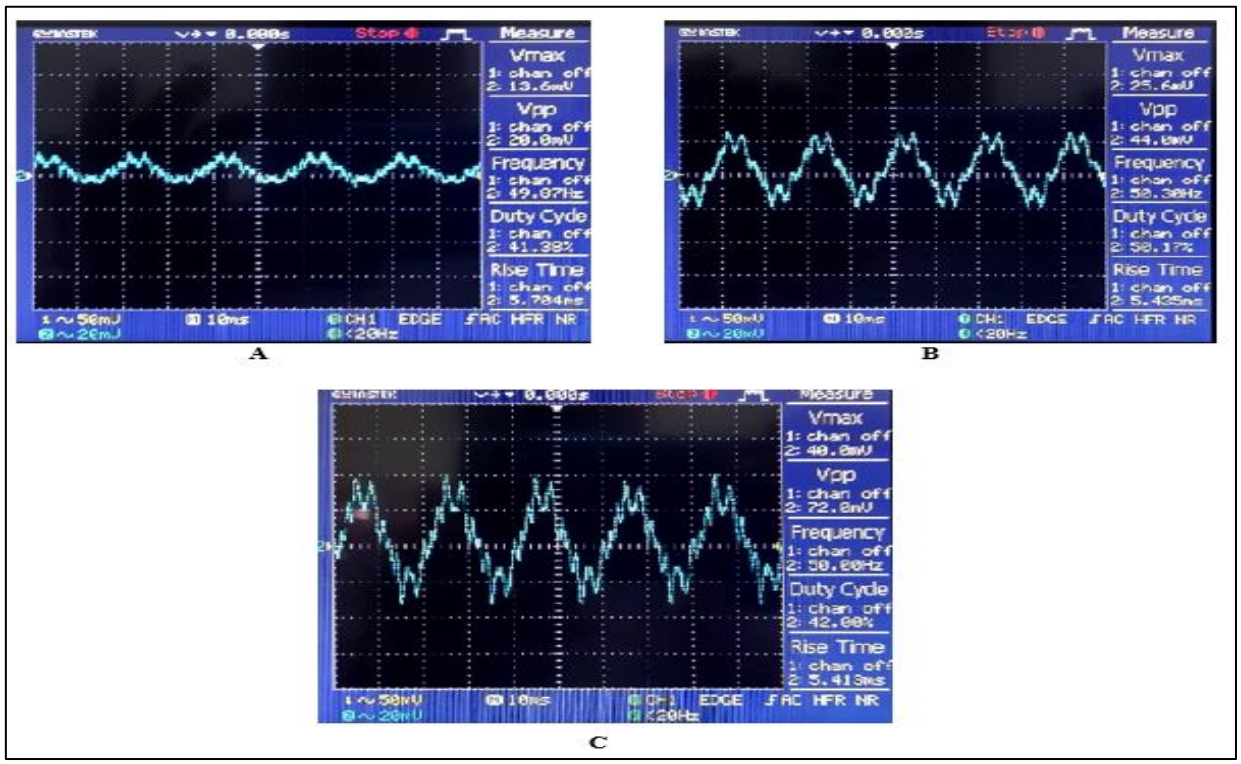

Figure III.18. Graphical curves of leakage current for the Transversely textured sample under different voltages: (A) 2KV, (B) 5KV, (C) 8KV.

- The dimension between the electrodes is 8 cm

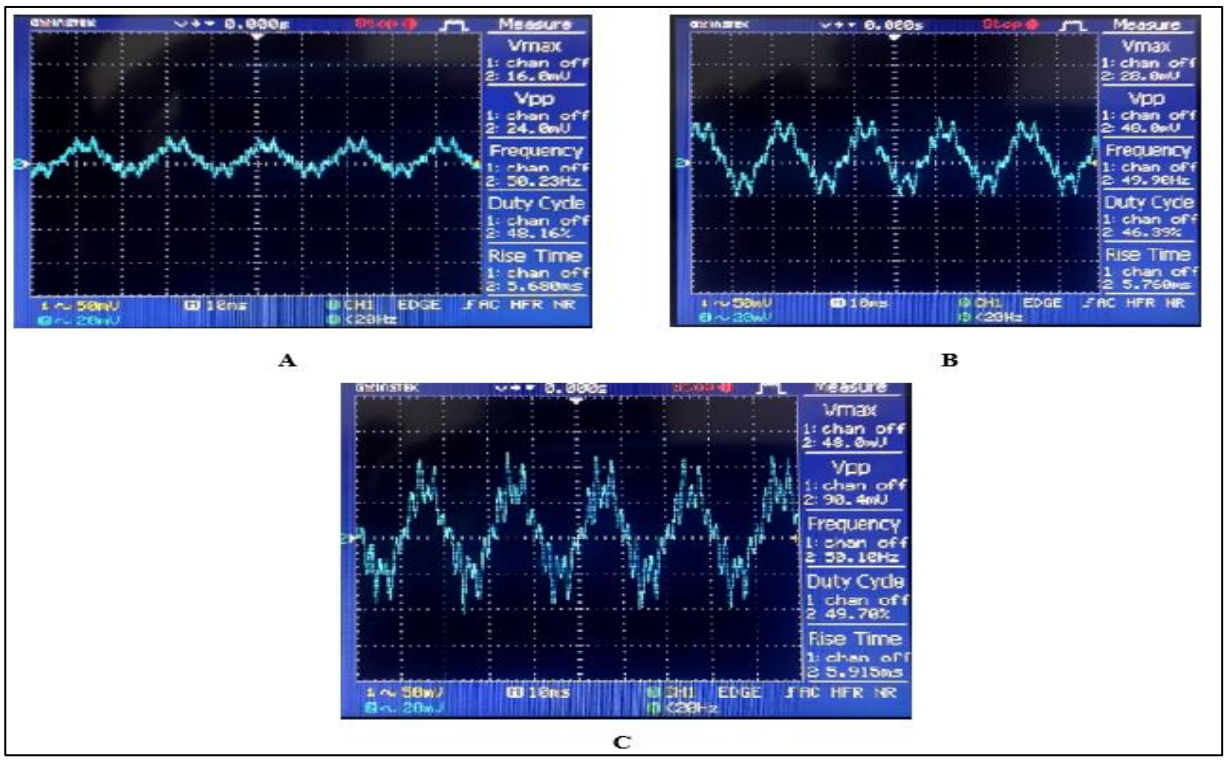

Figure III.19. Graphical curves of leakage current for the Transversely textured sample under different voltages: (A) 2KV, (B) 5KV, (C) 8KV.

- ✓ **Extraction**

The leakage current measurements for the three different surface textures (non-textured, longitudinally textured, and transversely textured) of the PLA+ insulator samples provide valuable insights into their insulation performance under high voltage conditions.

1. Non-textured Sample:

The non-textured sample exhibited the highest leakage current values among the three samples for both electrode distances (4 cm and 8 cm) and across all applied voltages (2 kV, 5 kV, and 8 kV). This indicates that the smooth surface of the non-textured sample is more susceptible to leakage currents, which can lead to increased energy dissipation and potential insulation failures.

2. Longitudinally Textured Sample:

The longitudinally textured sample showed significantly lower leakage current values compared to the non-textured sample. At both electrode distances and for all applied voltages, the leakage current values were reduced by approximately 80-90% compared to the non-textured sample. This substantial reduction in leakage current can be attributed to the increased leakage path length and the formation of parallel current paths due to the longitudinal surface texture.

3. Transversely Textured Sample:

The transversely textured sample also exhibited lower leakage current values compared to the non-textured sample, although slightly higher than the longitudinally textured sample. The reduction in leakage current ranged from 75-85% compared to the non-textured sample, depending on the electrode distance and applied voltage.

4. Effect of Electrode Distance:

As expected, increasing the distance between the electrodes resulted in lower leakage current values for all three samples. This is due to the increased length of the leakage path, which reduces the electric field strength and leakage current density.

Overall, the introduction of surface texture, particularly the longitudinal texture, significantly reduced the leakage current in the PLA+ insulator samples. The formation of parallel current paths and the increased leakage path length contributed to improved insulation performance by minimizing energy dissipation through leakage currents.

These findings highlight the potential benefits of incorporating surface texturing in polymer insulator design to enhance their electrical insulation properties and reduce energy losses. Further optimization of the texture design and long-term performance evaluation under various environmental conditions could lead to the development of more efficient and reliable insulation solutions for various applications, such as power transmission and distribution systems.

IV Conclusion

This experimental study investigated the performance of plastique (PLA+) insulator samples with different surface textures (non-textured, longitudinally textured, and transversely textured) under high voltage conditions using the inclined plane test.

Overall, the experimental results demonstrate the potential benefits of introducing surface texture to polymer insulators for enhancing their electrical insulation properties. The formation of parallel current paths and increased leakage path length in the textured samples contributed to improved performance against surface tracking, corrosion, and electrical discharges.

These findings provide valuable insights into the design and development of high-performance polymer insulators for various applications, such as power transmission and distribution systems. Further research and optimization of the surface texture design, as well as long-term aging studies, could lead to the development of more efficient and reliable insulation solutions.

GENERAL CONCLUSION

General Conclusion

This research investigated a novel approach to improving the performance of high voltage insulators through surface texturing. The proposed design involves introducing hemispherical protuberances on the insulator surface, taking advantage of the molding properties of silicone rubber used in polymeric insulators.

Theoretical analysis and geometrical calculations demonstrated that textured patterns, particularly contiguous hexagonal and intersecting hexagonal/square configurations, can increase the surface area and creepage distance of insulators. This reduces the surface electric field strength and current density, leading to lower power dissipation and inhibiting the formation of dry bands that can lead to insulator failure.

Extensive experimental studies were conducted, including inclined plane tests on textured and non-textured polymeric samples, as well as clean fog tests on prototype insulators with different shed configurations (7-shed and 5-shed designs). The results consistently showed that textured insulators exhibited lower leakage currents, reduced discharge activity, lower accumulated dissipated energy, and improved flashover performance compared to conventional smooth-surface insulators, across various pollution levels.

The superior performance of textured insulators was attributed to the increased heat dissipation efficiency facilitated by the textured surface, as well as the formation of parallel current paths that mitigate the damaging effects of dry band arcs. Additionally, the 5-shed prototype design demonstrated better performance than the 7-shed design, indicating the importance of optimizing the insulator profile in conjunction with surface texturing.

To further validate the technology, a natural pollution monitoring station was established in collaboration with industry partners, where 400 kV textured and conventional insulators were installed and energized for long-term monitoring and evaluation under real-world conditions.

Overall, this research presents a promising solution for enhancing the reliability and performance of outdoor insulation systems, particularly in polluted environments. The surface texturing approach offers a novel way to improve the pollution flashover performance of polymeric insulators, with potential applications in power transmission and distribution networks. However, continued research, optimization, and long-term performance evaluation under various environmental conditions are necessary for broader implementation of this technology.

BIBLIOGRAPHIC

Bibliographic

[1] **G. Leroy et all**, Les propriétés diélectriques de l'air et les très hautes tensions, Edition Ayrolles, Paris, France, 1984.

[2] **G. Riquel, E. SpanGenberg,** De la céramique au synthétique, EDF-Epure, N° 58, Avril 1998.

[3] S. VITET, La pollution des isolateurs, EDF-Epure, Juillet 1990.

[4] **Suwarno** et **ArioBasuki** et **F. Lendy** et **Sumedi**,Improvingoutdoor Insulator performances Installed coastal area using Silicone RubberCoating, 2012 IEEE International Conference on Condition Monitoring and Diagnosis ,23-27 September 2012, Bali, Indonesia.

[5] **K.Yamada, A. Hayashi, C. Saka, K.Sakanishi and R.Matsuoka** ,Improvement of Contamination Flashover Voltage Performance of Cylindrical Porcelain Insulators , Conference Record of the 2008 IEEE International Symposium on Electrical Insulation,09-12 June 2008.

[6] **Y. Zhu, K. Haji, H. Yamamoto, T. Miyake, M. Otsubo, C. Honda**, Distribution of Leakage Current on Polluted Polymer Insulator Surface, Annual Report Conference on Electrical Insulation and Dielectric Phenomena,2006.

[7] **M. Otsubo, T. Hashiguchi, C. Honda, O. Takenouchi, T. Sakoda, Y. Hashimoto**, Evaluation of insulation performance of polymeric surface using a novel separation technique of leakage current, IEEE Transactions on Dielectrics and Electric al Insulation., Vol. 10, pp. 1053-1060, 2003.

[8] **W.T. Starr,** Polymeric outdoor insulation, IEEE Transactions on Dielectrics and ElectricalInsulation., vol. 25, pp. 125-136, 1990.

[9] **M. Belkacem**, Diagnostic des isolateurs haute tension sous tension alternative 50Hz, Mémoire deMagister, Ecole Nationale Polytechnique, 2014.

[10] **F. Meghnefi, C. Volat**et **M. Farzaneh** « Temporal and FrequencyAnalysis of the LeakageCurrentof a Station Post Insulator during Ice Accretion », IEEE Transactions on Dielectrics and ElectricalInsulation Vol. 14, No. 6; pp 1-6 December 2007.

[11] **H.H. Kordkheili, H. Abravesh, M. Tabasi, M. Dakhem,** and **M.M. Abravesh** "Determining the probability of flashover occurrence in composite insulators by usingleakagecurrentharmonic components", IEEE Transactions on Dielectrics and ElectricalInsulation., Vol. 17, No. 2, pp. 502-512, 2010.

[12] **S. Chandrasekar, C. KalaivananetandA.Cavallini**, Partial dischargedetection as a tool to infer pollution severity of polymericinsulators, IEEE Transactions on Dielectrics and ElectricalInsulation.,Vol. 17, No. 1, pp. 1-12, February 2010.

[13] **O. O. Filho et J.A. Cardoso et D. R. de Mello**m ,The Use of Booster Sheds to Improve the Performance of 800 kV Multicone Type Insulatorsunder Heavy Rain, IEEE 2010 International Conference on High Voltage Engineering and Application,11-14 October 2010.

[14] Haddad, A., Waters, R., Griffiths, H., Chrzan, K., Harid, N., Sarkar, P., and Charalampidis, P., 'A new approach to anti-fog design for polymeric insulators', IEEE Trans. Dielectr. Electr. Insul., Vol. 17, (2): pp. 343-350, 2010

[15] Haddad, A. and Waters, R.T., Insulating Structures, UK Patent 2406225, 2003

[16] M. El A. Slama, M. Albano, A. M. Haddad, R. T. Waters, O. Cwikowski, I. Iddrissu, J. Knapper, and O. Scopes.2021 "Monitoring of Dry Bands and Discharge Activities at the Surface of Textured Insulators with AC Clean Fog Test Conditions" Energies 14, no. 10: 2914.https://doi.org/10.3390/en14102914.

[17] IEC 60587 :2007, “Electrical insulating materials used under severe ambient conditions. Test methods for evaluating resistance to tracking and erosion”, 2007.

[18] M. El-A. Slama, M. Albano, A. Haddad and R.T. Waters, “Dry-Band Discharges Dynamic at the Surface of SiR Textured Insulator During AC Inclined Plane Test”, Proceedings of the 21st International Symposium on High Voltage Engineering, Volume 2, Springer, 2019.

[19] IEC 60507 :1991, “Artificial pollution tests on highvoltage insulators to be used on a.c. systems”, 2014.

[20] Working Group C4.303, “Artificial Pollution Test for Polymer Insulators. Results of Round Robin Test”, Cigré, October 2013.

[21] BAHA Zakaria, BESSEI Abdedjabbar, Amelioration des performances d'isolation exterieure de l'isolateur composite Master's Degree in Electrical Engineering, University of Echahid Hamma Lakhdar - El Oued

APPENDIX

I The non- textured sample

Table.1. The table represent changes in voltage across the non- textured sample at varying dimension between the electrodes.

		1	2	3	Average	Corrected
The dimension between the electrodes is 2 cm	Corona effect	10.36	10.25	10.85	10.48	12.93
	Partial discharge	15.36	15.45	15.75	15.52	17.24
	Flashover voltage	19.73	19.50	19.45	19.56	21.73
The dimension between the electrodes is 6 cm	Corona effect	23.91	24.05	25.12	24.36	27.06
	Partial discharge	35.13	36.20	36.34	35.89	39.87
	Flashover voltage	47.14	35.95	46.36	43.15	47.94
The dimension between the electrodes is 10 cm	Corona effect	34.39	35.06	35.23	34.87	38.74
	Partial discharge	54.75	54.60	55.18	54.84	60.93
	Flashover voltage	65.53	65.36	66.40	65.76	73.07

- **Images:**

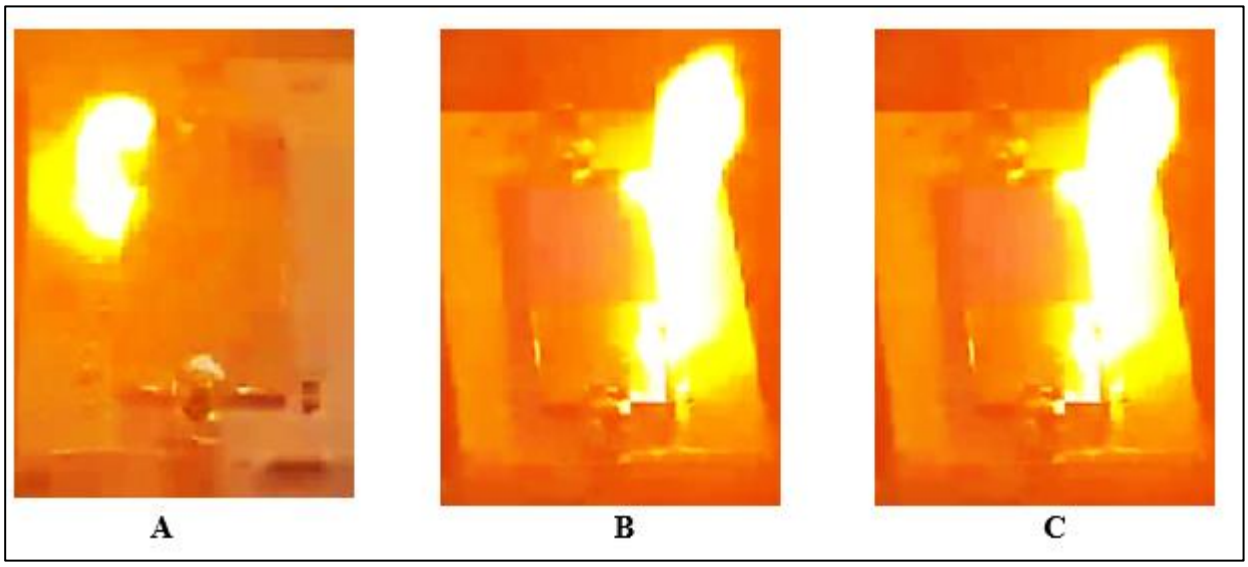

Figure. 1. Real images of the flashover voltage variation in the non- textured sample at different dimension betwee

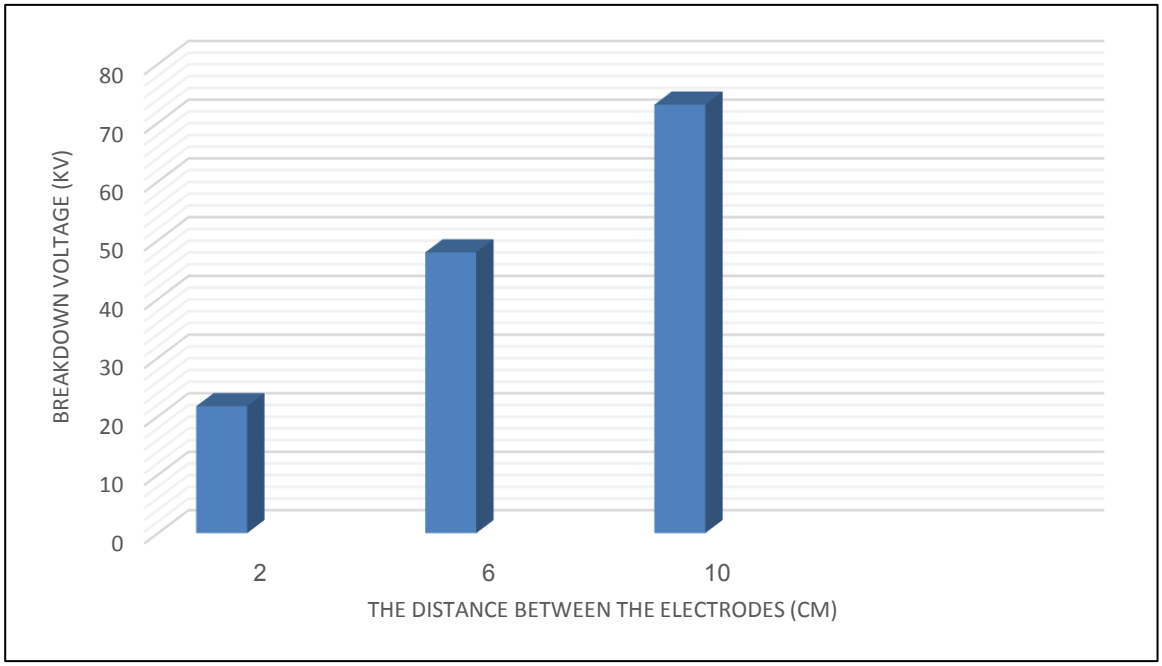

Figure. 2. Graph showing the change in flashover voltage in the non- textured sample.

II Longitudinally Textured Sample

Table.2. The tables represent changes in voltage across Longitudinally Textured Sample at varying dimension between the electrodes.

		1	2	3	Average	Corrected
The dimension between the electrodes is 2 cm	Corona effect	11.02	11.80	12.45	11.75	13.05
	Partial discharge	17.05	18.46	18.53	18.01	20.01
	Flashover voltage	18.84	20.96	21.02	20.28	22.53
The dimension between the electrodes is 6 cm	Corona effect	20.75	21.14	21.24	21.04	23.37
	Partial discharge	47.46	46.12	46.26	46.61	51.78
	Flashover voltage	55.25	55.86	55.65	55.58	61.75
The dimension between the electrodes is 10 cm	Corona effect	28.44	29.56	29.62	29.20	32.44
	Partial discharge	50.12	51.10	51.52	50.91	56.56
	Flashover voltage	67.50	65.55	66.46	66.50	73.88

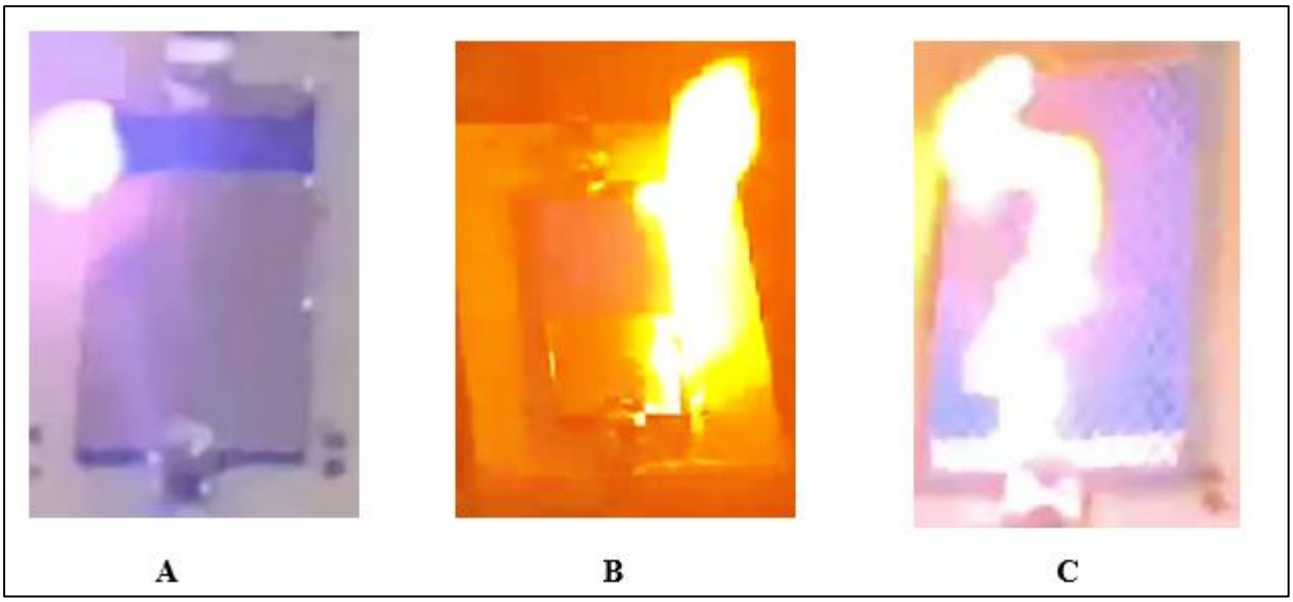

Figure. 3. Real images of the flashover voltage variation in the Longitudinally textured sample at different dimension between the electrodes: (A) 2 cm, (B) 6 cm, (C) 10 cm.

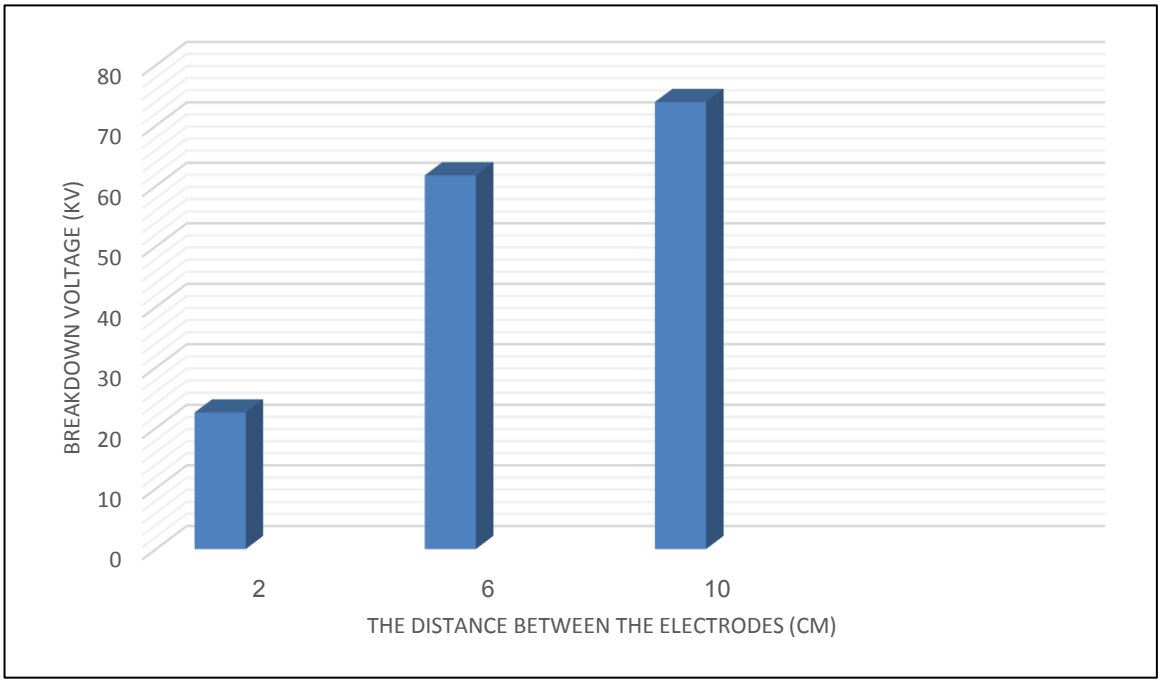

Figure. 4. Graph showing the change in flashover voltage in the Longitudinally textured sample.

III Transversely Textured Sample

Table.3. The tables represent changes in voltage across Transversely Textured Sample at varying dimension between the electrodes.

		1	2	3	Average	Corrected
The dimension between the electrodes is 2 cm	Corona effect	17.05	18.20	18.31	17.85	19.83
	Partial discharge	18.91	19.60	19.75	19.42	21.63
	Flashover voltage	21.41	21.80	21.85	21.68	24.08
The dimension between the electrodes is 6 cm	Corona effect	26.13	27.26	26.36	26.58	29.53
	Partial discharge	36.22	36.98	36.12	36.44	40.48
	Flashover voltage	48.50	49.12	50.02	49.21	54.67
The dimension between the electrodes is 10 cm	Corona effect	27.32	27.12	28.31	27.58	30.64
	Partial discharge	63.12	62.22	64.19	63.17	70.18
	Flashover voltage	73.52	74.88	73.02	73.80	82.00

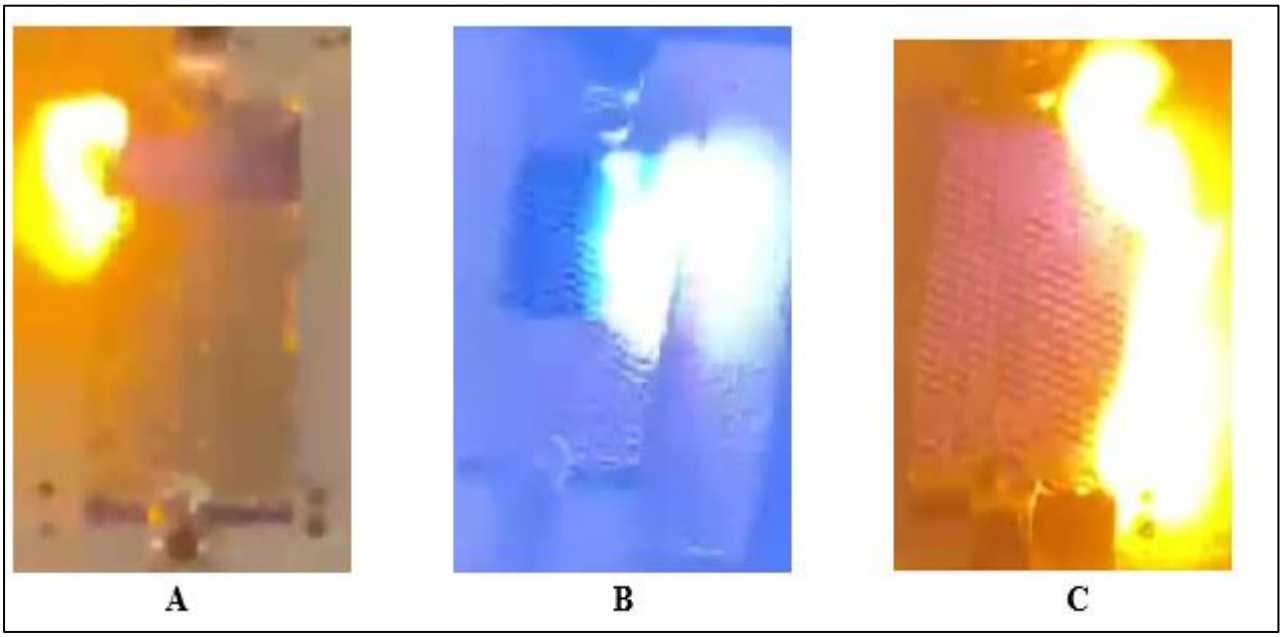

Figure. 5. Real images of the flashover voltage variation in the Transversely textured sample at different dimension between the electrodes: (A) 2 cm, (B) 6 cm, (C) 10 cm.

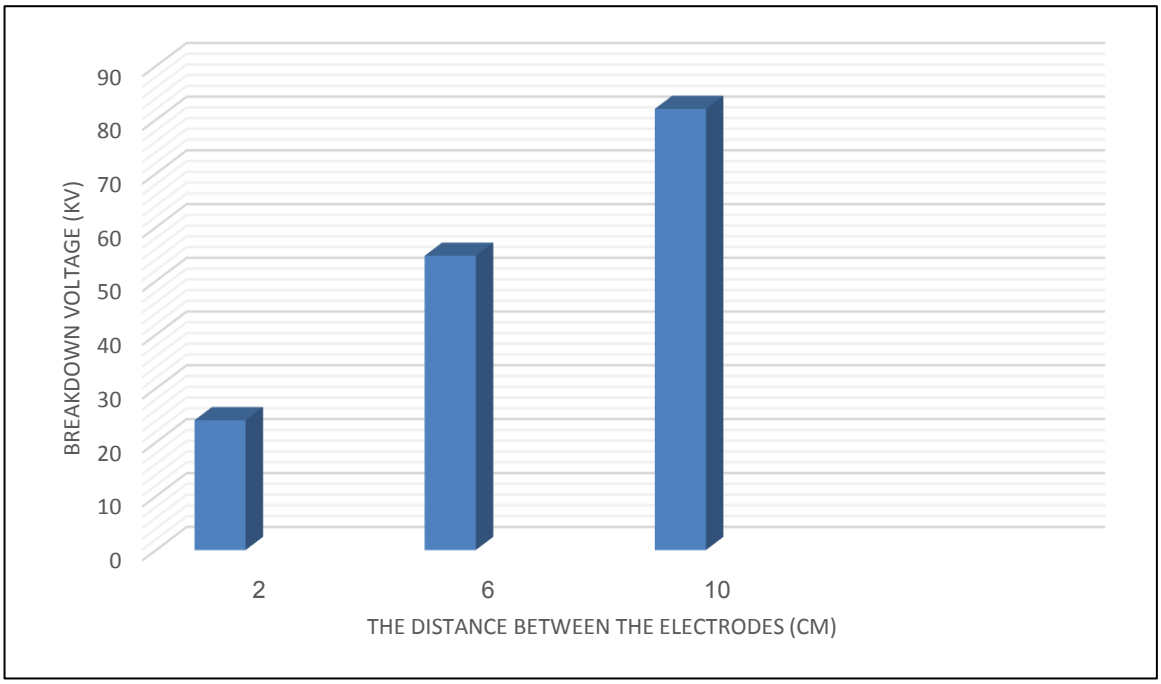

Figure. 6. Graph showing the change in flashover voltage in the Transversely textured sample.

IV Leakage current

IV.1. the non- textured sample

Table.4. The table represents the values of current leakage at different voltages

Voltage (KV)	The dimension between the electrodes is 2 cm	The dimension between the electrodes is 6 cm	The dimension between the electrodes is 10 cm
	The current leakage value at different voltages(µA)		
2	10.20	8.90	7.90
5	13.50	11	9.70
8	19.60	18.50	13

- The dimension between the electrodes is 2 cm

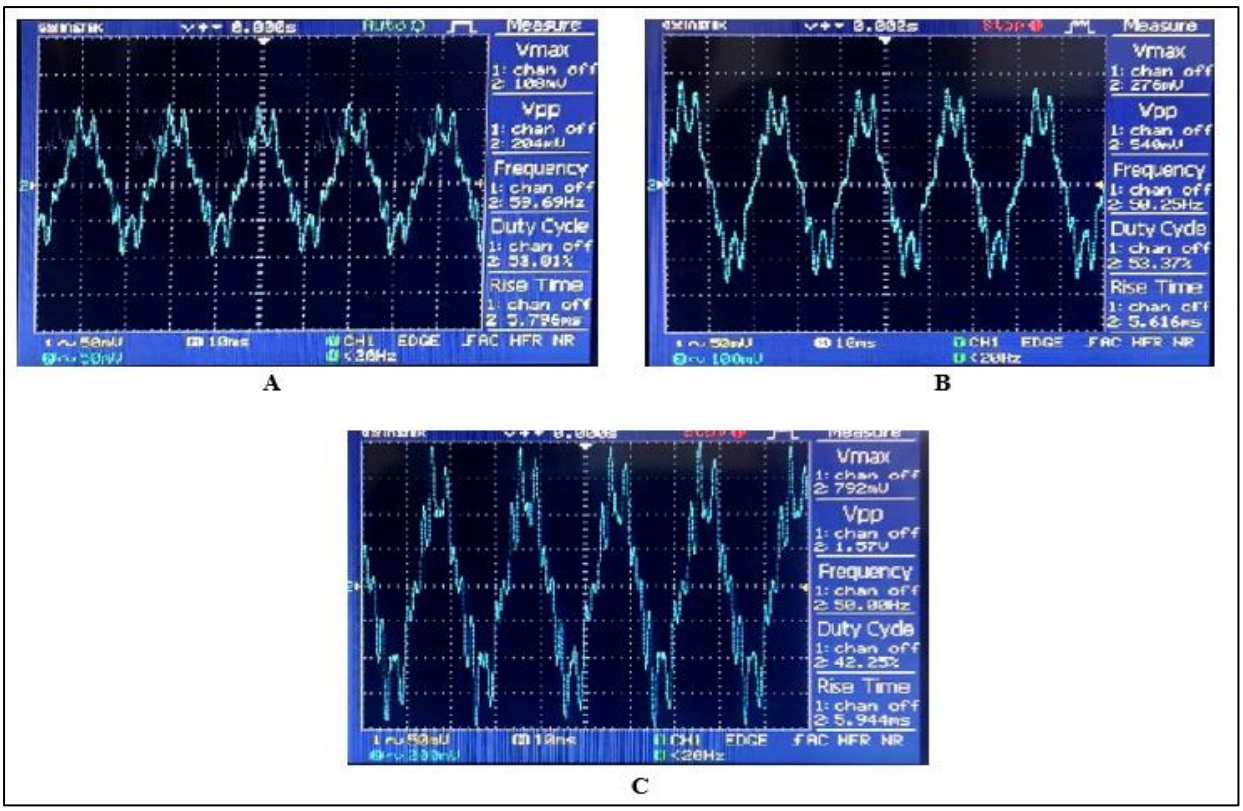

Figure. 7. Graphical curves of leakage current for the non- textured sample under different voltages: (A) 2KV, (B)5KV, (C) 8KV.

- The dimension between the electrodes is 6 cm

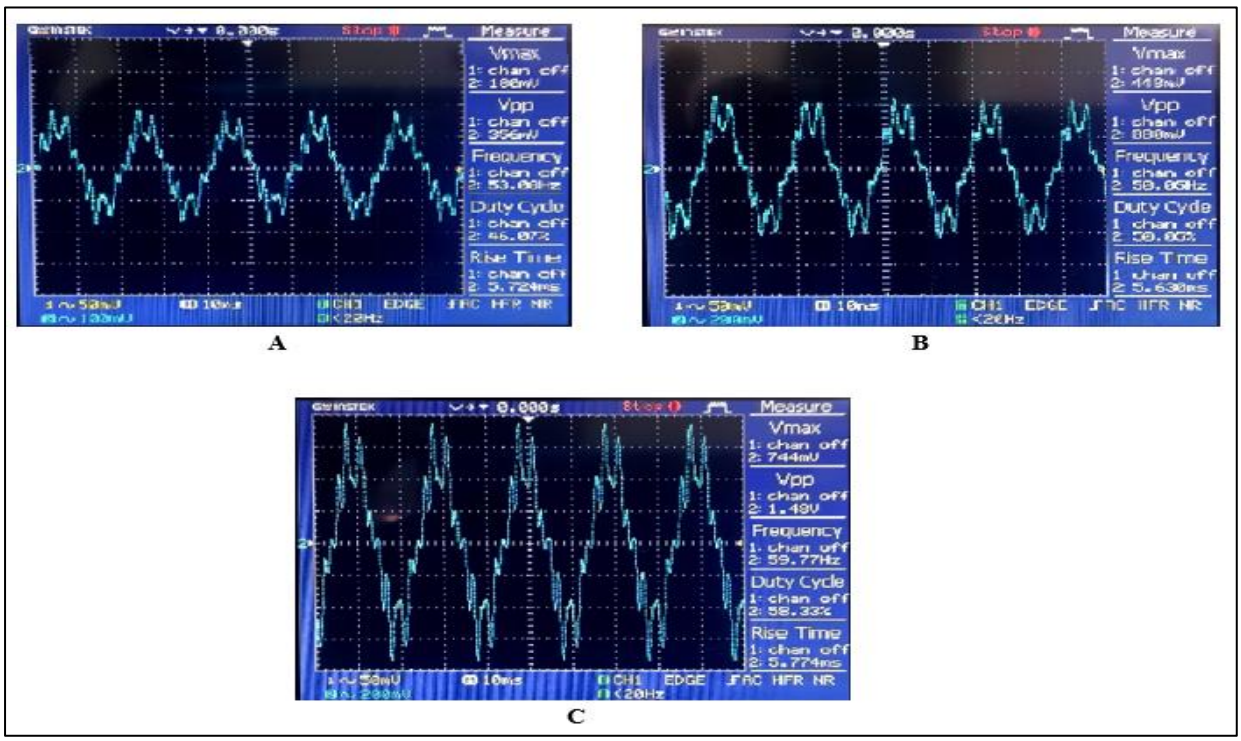

Figure. 8. Graphical curves of leakage current for the non- textured sample under different voltages: (A) 2KV, (B) 5KV, (C) 8KV.

- The dimension between the electrodes is 10 cm

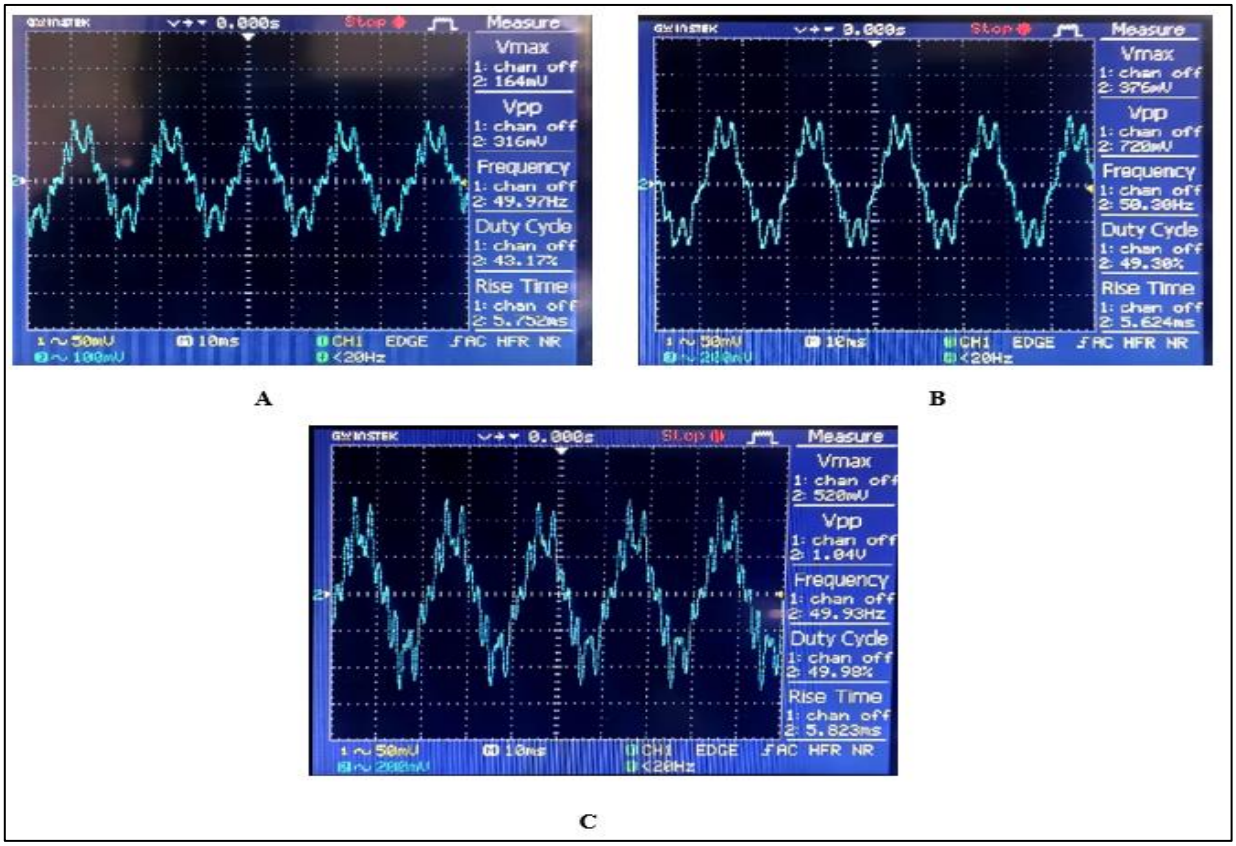

Figure. 9. Graphical curves of leakage current for the non- textured sample under different voltages: (A) 2KV, (B) 5KV, (C) 8KV.

IV.2. Longitudinally Textured Sample

Table.5. The table represents the values of current leakage at different voltages

Voltage (KV)	The dimension between the electrodes is 2 cm	The dimension between the electrodes is 6 cm	The dimension between the electrodes is 10 cm
	The current leakage value at different voltages (µA)		
2	1.20	1	0.88
5	3.20	2.50	2
8	5.05	3.80	3.20

- The dimension between the electrodes is 2 cm

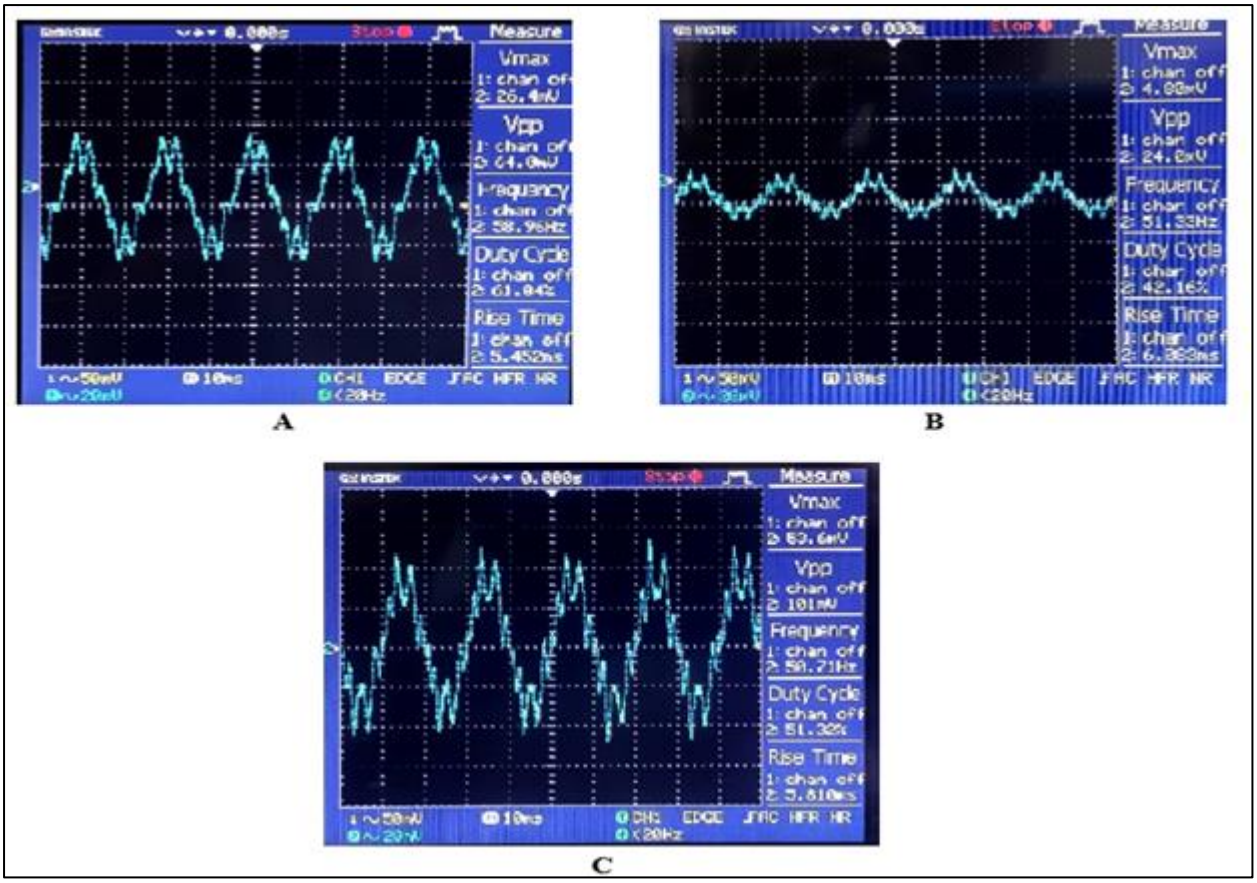

Figure. 10. Graphical curves of leakage current for the Longitudinally textured sample under different voltages: (A) 2KV, (B) 5KV, (C) 8KV.

- The dimension between the electrodes is 6 cm

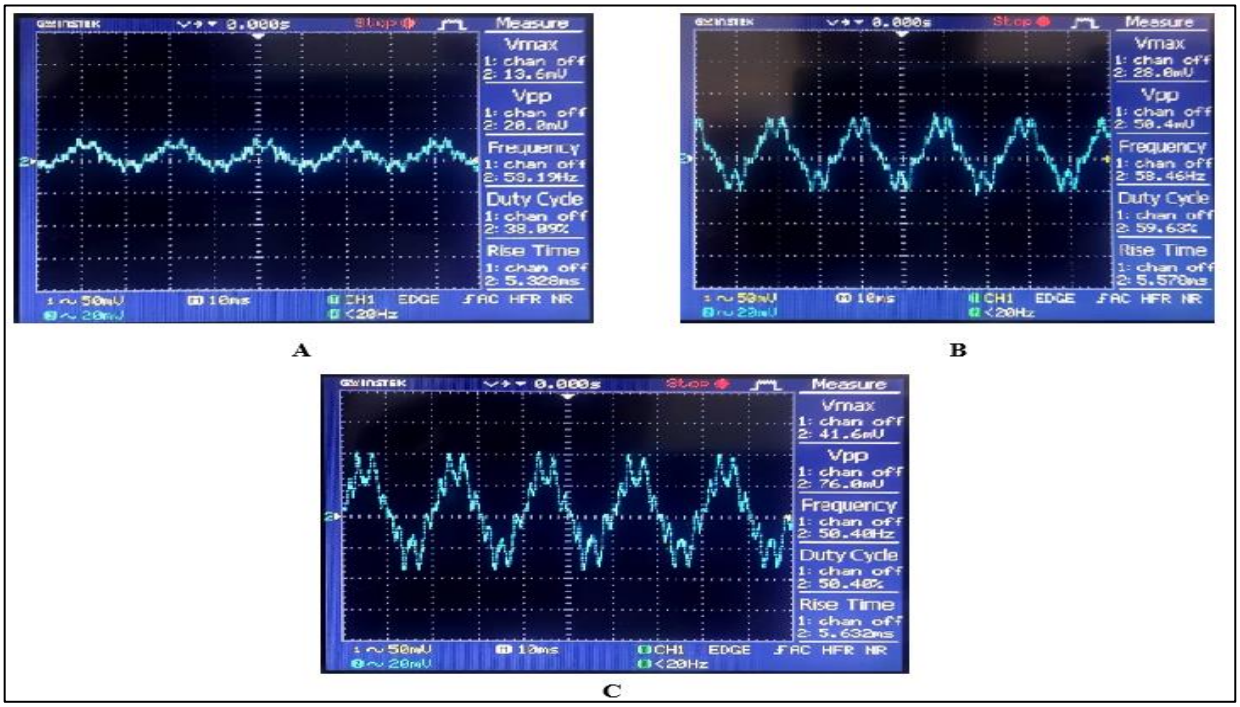

Figure. 11. Graphical curves of leakage current for the Longitudinally textured sample under different voltages: (A) 2KV, (B) 5KV, (C) 8KV.

- The dimension between the electrodes is 10 cm

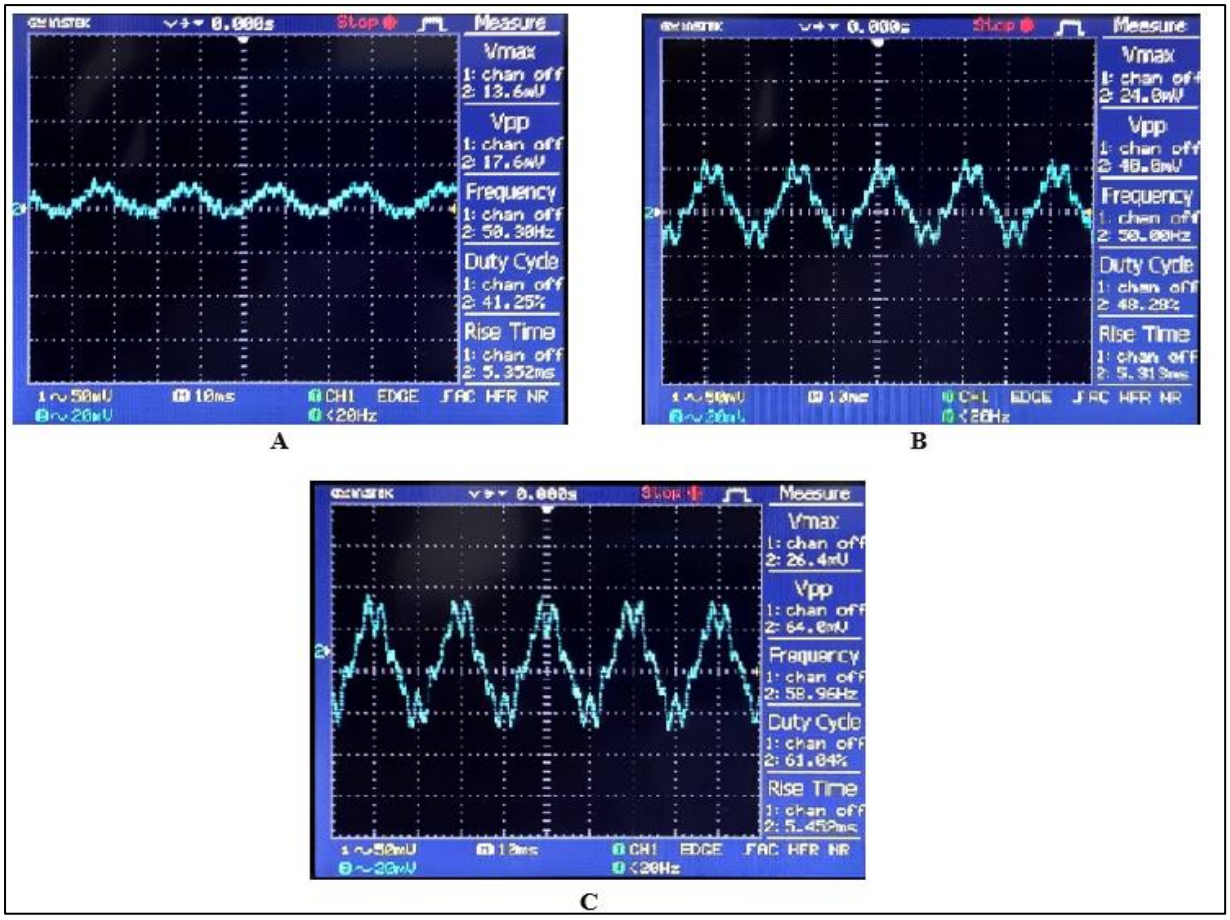

IV.3. Transversely Textured Sample

Figure. 12. Graphical curves of leakage current for the Longitudinally textured sample under different voltages: (A) 2KV, (B) 5KV, (C) 8KV.

Table.6. The table represents the values of current leakage at different voltages

Voltage (KV)	The dimension between the electrodes is 2 cm	The dimension between the electrodes is 6 cm	The dimension between the electrodes is 10 cm
	The current leakage value at different voltages(µA)		
2	1.40	1.32	1.20
5	3.20	2.60	2.40
8	5.80	4.50	4.50

- The dimension between the electrodes is 2 cm

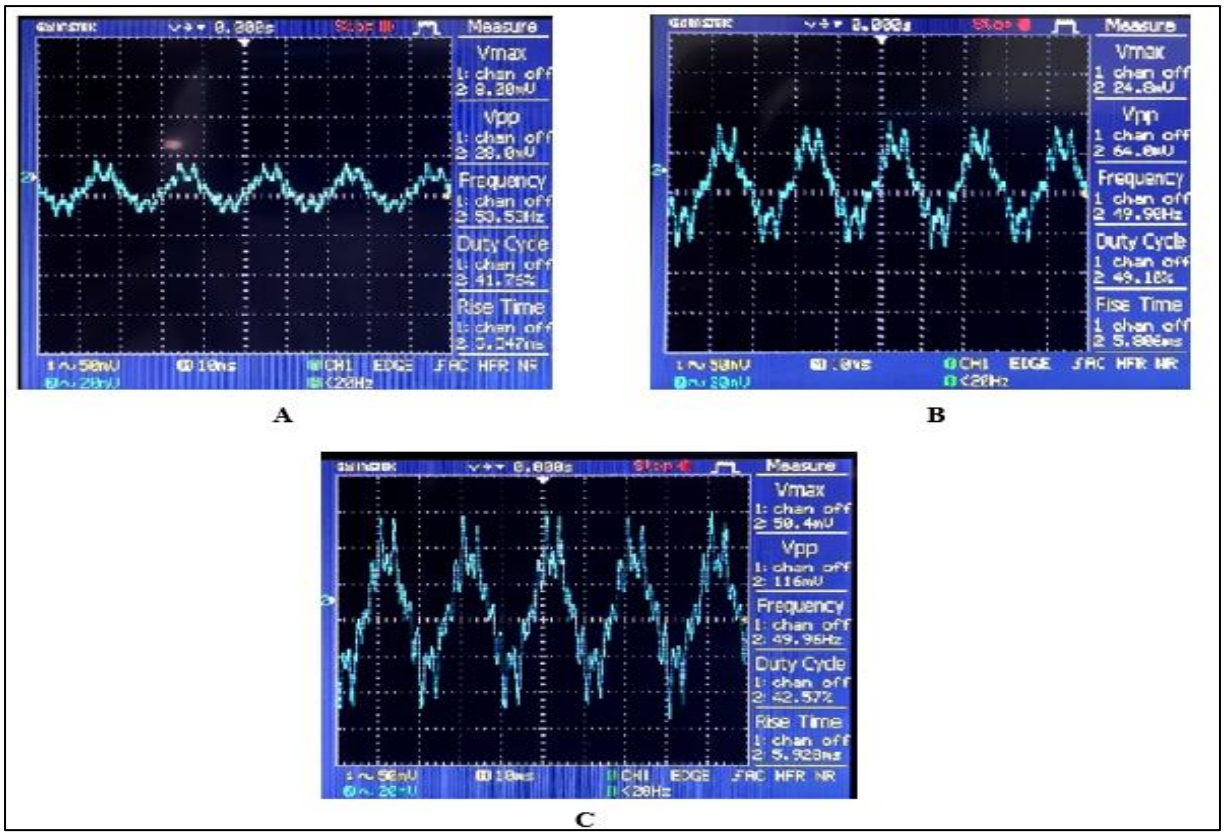

Figure. 13. Graphical curves of leakage current for the Transversely textured sample under different voltages: (A) 2KV, (B) 5KV, (C) 8KV.

- The dimension between the electrodes is 6 cm

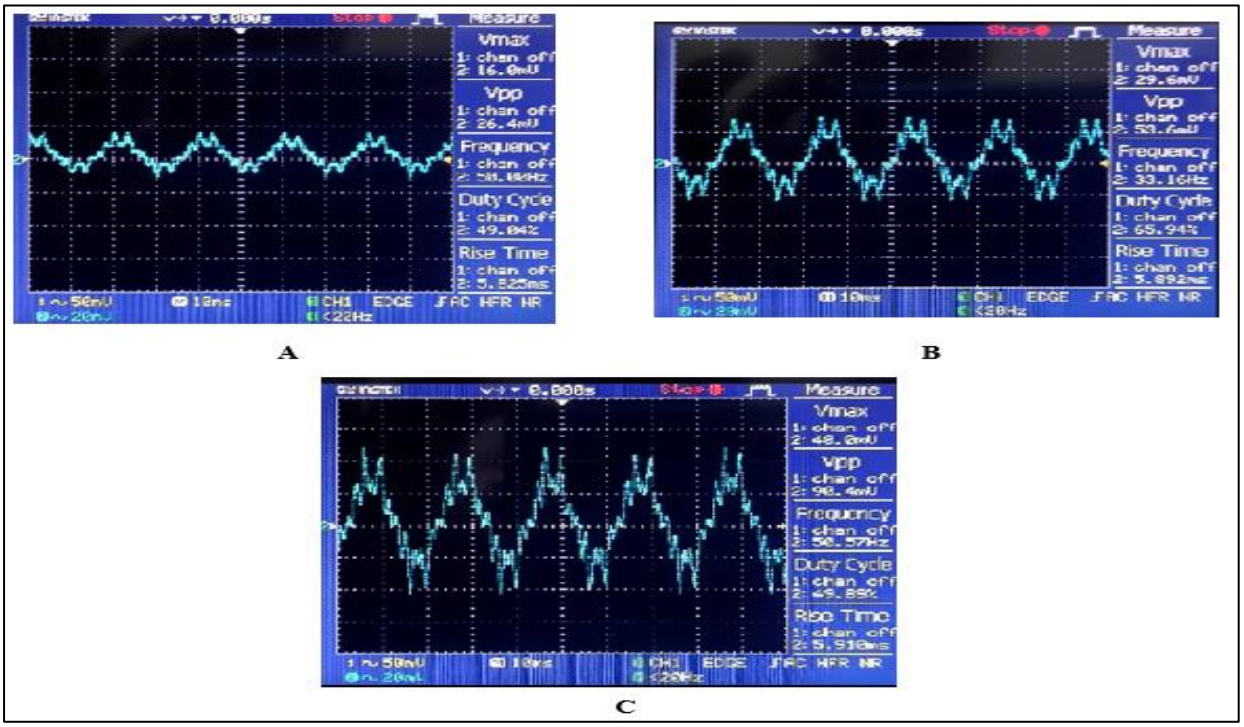

Figure. 14. Graphical curves of leakage current for the Transversely textured sample under different voltages: (A) 2KV, (B) 5KV, (C) 8KV.

- The dimension between the electrodes is 10 cm

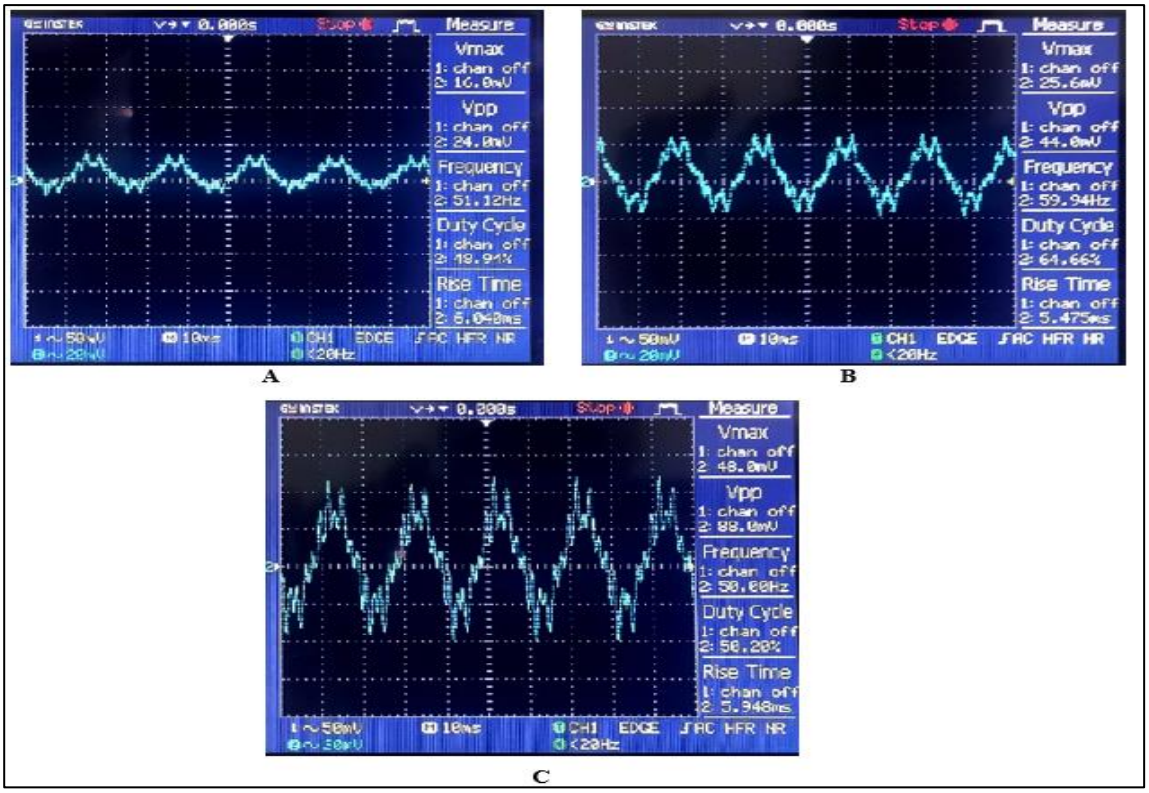

Figure. 15. Graphical curves of leakage current for the Transversely textured sample under different voltages: (A) 2KV, (B) 5KV, (C) 8KV.